Science of the Total Environment 969 (2025) 178858

Contents lists available at ScienceDirect

Science of the Total Environment

journal homepage: www.elsevier.com/locate/scitotenv

Divergent regional volume growth responses of Scots Pine and Oak stands to climate change in Europe

Carl Vigren [a,*], Sonja Vospernik [b], Xavier Morin [c], Maude Toïgo [c], Kamil Bielak [d], Felipe Bravo [e], Michael Heym [f], Magnus Löf [g], Maciej Pach [h], Quentin Ponette [i], Hans Pretzsch [j]

[a] Swedish University of Agricultural Sciences (Umeå), Sweden
[b] University of Natural Resource and Life Sciences Vienna, Austria
[c] University of Montpellier, France
[d] Warsaw University of Life Sciences, Poland
[e] Universidad de Valladolid, Spain
[f] Bavarian Institute of Forestry, Germany
[g] Swedish University of Agricultural Sciences (Alnarp), Sweden
[h] Uniwersytet Rolniczy im Hugona Kołłątaja w Krakowie, Poland
[i] Catholic University of Louvain, Belgium
[j] Technische Universität München, Germany

HIGHLIGHTS

- 1 km^2 gross volume growth forecasts for stands of Oak, Scots Pine under RCP 4.5/8.5
- Forecast reductions for Scots Pine stands larger in southern than northern Europe
- Parts of southern Europe show Oak stand growth increases relative to historical

GRAPHICAL ABSTRACT

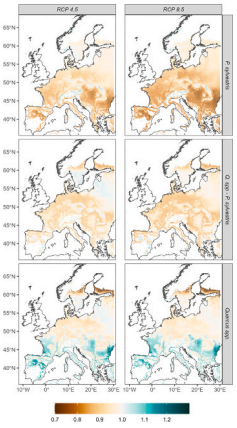

ARTICLE INFO

Editor: Alessandra De Marco

Keywords:
Oak

ABSTRACT

European climatic change has been proposed to induce many changes to forests, about factors such as tree species distributions, site productivity, groundwater availability, outbreaks of forest pests, and damage from wind-breakage of trees. Novel approaches to empirical tree growth modelling using re-measurements over large

* Corresponding author.
E-mail addresses: carl.vigren@slu.se (C. Vigren), sonja.vospernik@boku.ac.at (S. Vospernik), xavier.morin@cefe.cnrs.fr (X. Morin), maude.toigo@agro-bordeaux.fr (M. Toïgo), kamil_bielak@sggw.edu.pl (K. Bielak), felipe.bravo@uva.es (F. Bravo), michael.heym@lwf.bayern.de (M. Heym), magnus.lof@slu.se (M. Löf), rlpach@cyf-kr.edu.pl (M. Pach), quentin.ponette@uclouvain.be (Q. Ponette), hans.pretzsch@tum.de (H. Pretzsch).

https://doi.org/10.1016/j.scitotenv.2025.178858
Received 12 November 2024; Received in revised form 8 February 2025; Accepted 12 February 2025
Available online 26 February 2025

Pine
Climate change
Forest growth model
RCP 4.5
RCP 8.5

climatic gradients capture variability associated with long-term climatic conditions as well as weather during the growth period.

Using the latest version of the individual tree-based forest simulator, PrognAus, which has been outfitted with a climate-sensitive basal area increment module, we forecast growth of trees in pure and mixed stands of Pinus sylvestris L. and Quercus spp. across a network of 23 European sites between 2017 and 2100 under current climate and RCP 4.5 and RCP 8.5 climatic scenarios. By training a stand-level static reduced model (SRM) from these local level results, we forecast widespread future growth changes for stands of Pinus sylvestris and Quercus spp. across Europe.

Our SRM predicts stand gross-volume relative growth (ratio of the gross volume production in a given growth year to the gross volume production until the start of the growth year) with a generalized additive mixed model (GAMM). We decomposed overall growth into tensors capturing variation associated with stand species mixture type (pure P. sylvestris, mixed P. sylvestris- Q. spp., pure Q. spp.), age, and weather conditions during the growth year and the preceeding year. Wall-to-wall predictions based on the SRM are presented for a high-resolution 30-arcsecond grid spanning most parts of Europe.

1. Introduction

Climate change mitigation and adaptation are current issues of major global concern. Within the United Nations Framework Convention on Climate Change (UNFCCC, 1992), the sector Land Use, Land-Use Change, and Forestry (LULUCF) has been considered of outstanding importance due to its large potential for mitigating climate change, despite major technical challenges to assessing the sector's contribution to overall greenhouse gas budgets remaining (Shukla et al., 2019). Some parties to the UNFCCC, such as the member states of the European Union, have recently decided upon specific measures to increase the carbon sink in their LULUCF sectors pursuant to limiting global average temperature increases below 1.5 °C above pre-industrial level (European Union, 2023; UNFCCC, 2021). The impact of forest management may be substantial in countries with large forest holdings and has been intensively debated, particularly in countries where forests and forestry are instrumental components of fossil fuel abatement strategies (Kauppi et al., 2022; Petersson et al., 2022; Skytt et al., 2021). Assisted migration to mitigate or avoid losses is frequently suggested, however few studies approach the subject of species suitability or species potential to deliver forest ecosystem services through a continuous time-frame (e.g. Mauri et al., 2023; Wessely et al., 2024).

Still, Scots Pine (*Pinus sylvestris*) may experience notable contractions throughout the northern European Plain without commensurate range expansion taking place already during near future (2041–2060) periods from moderate future scenarios such as the CMIP6 SSP2.45 (Dyderski et al., 2025). This moderate scenario corresponds to an end-of-century level of 4.5 Wm^{-2} net increase in radiative forcing relative to the 1750 historical baseline. Meanwhile, large northward expansions of Sessile (*Quercus petraea* (Matt.) Liebl.) and Pedunculate Oak (*Quercus robur* L.) into the boreal forest belt are expected (ibid.).

Equating potential distributional change into commensurate changes in the productive capacity of species is not without issue as it must be considered that conditions for growth are continuously changing due to, e.g., stand management, changing weather patterns, nutrient deposition (anthropogenic or other) and follow-on legacy effects.

Thus, future environmental conditions constitute central input to modelling future growth, and are frequently obtained as aggregations from suitable ensembles of general circulation models, *GCMs* (Sanderson et al., 2015). *GCM* results are based on scenarios including future emissions and uptakes of greenhouse gases. Such scenarios include the SRES (IPCC Special Report Emissions Scenarios) and the representative concentration pathways (*RCPs*). Newly published *Shared Socioeconomic Pathways* link previous and new *RCPs* to narratives of societal development. The results from climate experiments are therefore ordered by GCM (model), initial conditions, spin-up phase, physics, and scenario – frequently coordinated under CMIP (*Coupled Model Intercomparison Project*) auspices. As a result, variation between GCM results can be expected for the same scenario, the effects of which for studies on potential future tree species distributions are explored further by *i.a.* Goberville et al. (2015).

The *RCPs* depart from a common baseline of about 380 ppm CO_2 in 2005 before diverging to different paths. As an example, the RCP 4.5 scenario (end-of-century levels of net change in radiative forcing since 1750 at 4.5 Wm^{-2}) is consistent with a future in which carbon emissions peak mid-21st-century and then decline to be roughly halved by 2100 for an average CO_2 concentration of ca. 540 ppm. In contrast, RCP 8.5 assumes continued large greenhouse gas emissions, leading to average CO_2 concentrations during the 21st century being about 940 ppm (IPCC, 2013, Table All.4.1). The explored RCP scenarios (4.5, 8.5) can be best compared to CMIP6 scenarios SSP2.45 and SSP5.85 or SSP4.85.

Increases in the atmospheric concentration of carbon dioxide is the largest contributor to the total amount of radiative forcing since 1990 (NOAA, 2024). Concomitant productivity increases, 'carbon fertilisation', sensu Norby et al. (2005), does appear to have had some impact already. Argles et al. (2023) suggest that between 1973 and 2017 it could have contributed to about 7 % increased growth. It can be hypothesized that plant growth at the same time would instead be hindered due to, e.g., poor adaptation, nutrient imbalances, and shortage of water, suggesting that any positive effects may be transient (Jonard et al., 2015; Sperry et al., 2019; Terrer et al., 2018). For example, Pretzsch et al. (2014) found that climatic conditions alone were insufficient to reproduce observations of increased growth in young stands of *Picea abies* L. (H. Karst.) and *Fagus sylvatica* L. in Central Europe, but that the combined effect of climate, enhanced atm. [CO_2] and increasing levels of nitrogen deposition did.

A later study (Pretzsch et al., 2023a) identified time-trends across Europe (1975–2017) for a climatic index correlated with site productivity (Paterson, 1956): particularly strong trends over time were found for the Scandinavian peninsula (positive), and the northern Iberian peninsula (negative), whereas at intermediate latitudes and the Balkans only a weak positive trend was identified. Nemani et al. (2003) found growth to be radiation-temperature limited (Fennoscandia), radiation limited (intermediate latitudes), or temperature-water limited (Spain) (ibid., Fig. 1). During the same period, changes in temperature, vapor pressure deficit and solar radiation contributed to increases in net primary production, especially in central Europe (ibid., Fig. 2). Overall, a review by Boisvenue and Running (2006) found support for the hypothesis that forest growth had increased during the latter half of the 20th century for "Northern Europe, most of Central Europe, some parts of Southern Europe".

As environmental factors continue to change, modelling can be used for investigating the consequences on growth across different climatic projections (Fontes et al., 2010). Matías et al. (2017) observed that basal area growth of *Pinus sylvestris* L. populations had increased rapidly between 1960 and 2011: however, the slope of this increase weakened towards higher latitudes and lower altitudes. The SRES-A1B scenario was projected to entail large increases across the entire latitudinal distribution range of *P. sylvestris*, but increases were expected to be smaller at low altitudes, especially approaching the mid-21st century. Bergh

et al. (2010) suggested relative increases in gross stem volume production for *P. sylvestris* in southern Sweden of up to 20 % under the SRES-A4 scenario compared to a reference climate (1961–1990); however, they expected increasing water stress throughout southern Sweden. More recent work suggests some mortality stemming from summer drought stress to *P. sylvestris* in southern Sweden may be offset by decreasing late winter and spring drought under future climatic scenarios (RCP 2.6, 4.5, 8.5) (Aldea et al., 2024).

Using the FINNFOR process-based model (Kellomäki and Väisänen, 1997), Briceño-Elizondo et al. (2006) predicted large growth increases under climate change in northern Finland and moderate increases in southern Finland. Similar results were obtained by Kellomäki et al. (2018) with the model SIMA. Bouwman et al. (2021) used 3-PG_{mix} (e.g., Forrester and Tang, 2016) to predict the growth of *P. sylvestris*, and *Quercus* spp. (i.e. *Q. robur* L. & *Q. petraea* (Matt.) Liebl.) across the Netherlands up until 2050, projecting declining levels of growth, particularly for *Q.* spp.

Nölte et al. (2020) found limited increases to stem growth (3–8 %) for *Q. petraea* in south-west Germany under an 80-year simulation with the RCP 4.5, RCP 8.0 scenarios, mostly attributed to lengthening of the growing season. More generally for Germany, Gutsch et al. (2016) used static reduced models (*SRMs,* i.e. simplifications of complex models) of a process-based model and found that the net primary production of *P. sylvestris* and *Q.* spp. would increase during a near future period (2031–2060) following scenarios based on the SRES-A1B (roughly corresponding to RCP 6.0), particularly on water-limited or high-elevation sites, and that in areas with limited change, uncertainty increased dramatically. Further south, Ameztegui et al. (2017) projected decreases in growth for *Q.* spp. in northeast Spain, and suggested that moderate thinning could be a means to mitigate productivity losses due to water stress.

Several of the studies referred to above provide a general picture of declining growth in stands of *P. sylvestris* and *Q.* spp. in southern and central Europe, but of increasing growth in northern Europe under future climatic conditions. However, the studies are based either on i) process-based models, or ii) signal-transfer hybrid models sensu Fontes et al. (2010). Spatial evaluations of growth under different climatic scenarios with statistical hybrid models outfitted with functional relationships to climatic variables are scarcer. However, by coupling a climatic modulator to stand-level increments from an individual tree model, Vallet and Perot (2018) found only minor changes for stands of *Q. petraea* or *P. sylvestris* in Orleans, France. The authors predicted that both species would experience slight increases in basal area increment during the first half of the 21st century, but that the increment of *Q. petraea* would stabilise around its historical level during the second half of the 21st century (under RCP 2.6, 4.5 and 8.5). *P. sylvestris* was forecast to undergo a slight decline of growth, which stabilised at around 95 % of the historical level. In contrast, Goude et al. (2022) suggested, based on a + 2° Kelvin 20-year pulse scenario, that temperature is currently limiting basal area growth of *P. sylvestris* on northern sites of Sweden, whereas water deficit hinders growth along the south-eastern coastline of Sweden (ibid, Fig. 7a). Finally, Vospernik et al. (2024) projected broad reductions across Europe in development of standing volume in unmanaged stands of *P. sylvestris* and *Q.* spp. under the RCP 4.5 and RCP 8.5 scenarios with a linear mixed model. However, this approach was unable to inspect temporal trends and was limited to forecasts for a limited number of sites, although generalised results across latitudinal and longitudinal gradients were presented.

Almost all the reviewed articles have had a local or regional focus. Few studies address changing growth conditions across larger geographical scales, although studies like Vospernik et al. (2024) address changes for sites distributed across a large portion of Europe. As mentioned in this study (ibid.), basal area may be the most climatically impacted growth component of trees and stands. We thus hypothesize that by parametrizing a static reduced model from the site-specific results obtained in Vospernik et al. (2024), interesting patterns of growth changes across Europe might be revealed, which could follow from regional differences in anticipated climate change that go beyond simple interpolations across latitudes and longitudes. Through static reduced modelling in this context, we could generalise the results from a complex growth model through a simpler model, which, however, still could apply fine-grained local level inputs of climate variables, available from RCP projections.

Thus, the main objective of this study was to generalise the results

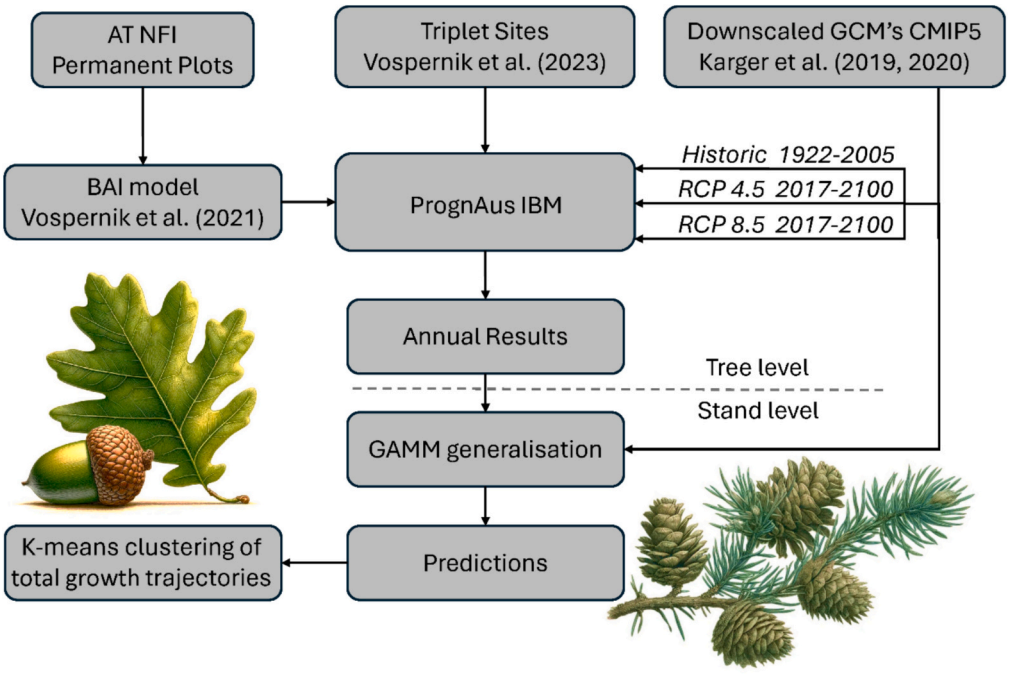

Fig. 1. An overview of the workflow we applied. BAI stands for basal area increment, CMIP5 for Coupled Model Intercomparison Project Phase 5, GCM for General Circulation Model, IBM for Individual Based Model, and AT NFI for Austrian national forest inventory.

based on forecasts for monospecific and mixed stands from Vospernik et al. (2024) to provide a wall-to-wall map across Europe of the growth consequences for different stand types of *P. sylvestris* and *Q.* spp. under the scenarios RCP 4.5 and RCP 8.5, whilst contrasting this against the historical period 1922–2005. These results could be important for discussions about suitable management of European forests for mitigating climate change, and for adapting forestry to the consequences of changing conditions.

2. Material and methods

Based on the results from Vospernik et al. (2024) we obtained tree level data from plots for *P. sylvestris*, *Q.* spp., and their mixture for different locations across Europe (see 2.1). For these stands, climate-sensitive forecasts were made at individual tree level with the latest version of *PrognAus* (Monserud and Sterba, 1999; Nachtmann, 2005; Vospernik, 2021), and the results subsequently aggregated to the stand level.

We modelled the stand level outputs from *PrognAus* as a discrete annual process using climatic variables developed within the *CMIP5* project headed by the World Climate Research Programme (Taylor et al., 2012). For this purpose, we applied a flexible generalised additive mixed model, *GAMM* (Hastie and Tibshirani, 1986). With the estimated model, we made wall-to-wall predictions across Europe on a 30-arcsecond resolution grid (east-west resolution ~0.93 km at equator, ~0.46 km at 60°N). Areas with climatic conditions too far from the downscaled ensemble data experienced at the sites in Vospernik et al. (2024) were excluded to avoid model extrapolation (white areas, Fig. 9). In a final step, the results were clustered to obtain more easily interpretable patterns of growth change of *P. sylvestris* and *Q.* spp. stands across Europe. Fig. 1 provides an overview of the methodological approach applied.

In the following, we first give a brief summary of the data and methods applied in the study by Vospernik et al. (2024). Then, we describe the developed Generalised Additive Mixed Model, *GAMM*, and relevant input data from the climatic scenarios. Last, we describe how our outputs were clustered.

2.1. An overview of the application of PrognAus for individual sites

As described in Pretzsch et al. (2020) 23 triplet sites were inventoried in late 2017. Each 'triplet' is a plot with one single-layered, even-aged sub-plot at maximum density each of *P. sylvestris*, *Q.* spp., and their mixture *P. sylvestris* – *Q.* spp. Plots were situated on a gradient from xeric/nutrient poor to mesic sites of moderate nutrient status. For each tree diameter at breast height (1.3 m), tree height, crown-length, and local coordinates were recorded. Stand ages were computed from a cored subsample of trees spanning the diameter-distribution. For detailed information on the triplets we refer to previous studies (Engel et al., 2021; Pretzsch et al., 2020; Steckel et al., 2020; Vospernik et al., 2023, 2024).

For summary information on the initial conditions in the subset of 15 triplets used in this study, we refer to Table I in the supplementary data of Vospernik et al. (2024).

As in our previous study, i.e. Vospernik et al. (2024), we do not differentiate between *Q. petraea* and *Q. robur*. This is because the species are not differentiated in *PrognAus* – the individual tree-based model we build the study on, and furthermore, the species were not distinguished by the inventory of the study sites. Across most of their ranges throughout Europe, the species are sympatric, and can interbreed with fertile offspring (*Q. x rosacea* Bechst.) (Petit et al., 2004).

The development of plots, assumed to be unmanaged, was then forecast for different climatic scenarios (Historical, *RCP 4.5*, *RCP 8.5*) with single-year time steps with the latest version of the *IBM PrognAus,* outfitted with the climate-sensitive basal area increment model

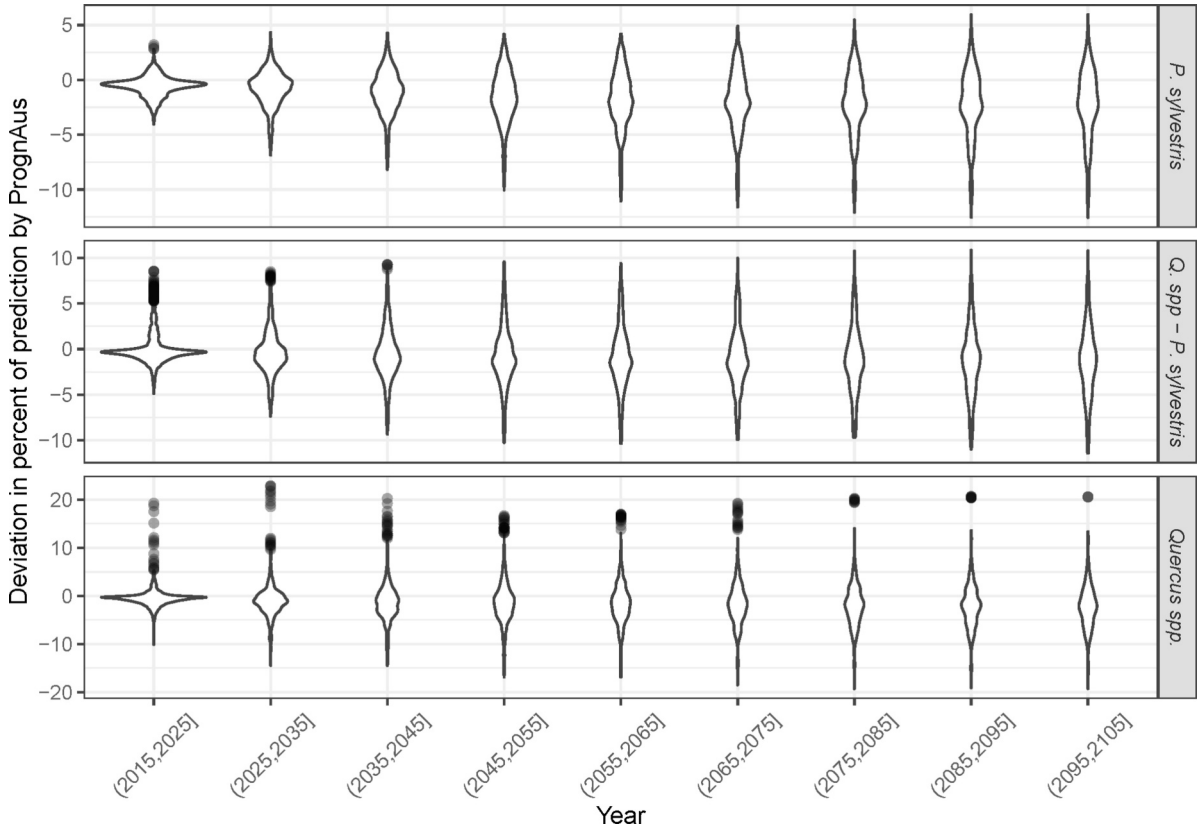

Fig. 2. Violin plots depicting the density of deviations of the GAMM from results of the PrognAus IBM simulations. Outliers >3 standard deviations from the mean are plotted as points. Note the different scales for the different species groups.

developed by Vospernik (2021). Other variables were forecast with routines which were not developed to be climate-sensitive: height increment (Nachtmann, 2005); crown ratio (Hasenauer and Monserud, 1996) and mortality (Monserud and Sterba, 1999). Ingrowth was not considered, as ingrowth in the stands utilised for the study was expected to contribute very little to overall growth. Note that Nachtmann's (ibid.) height increment functions do not depend on basal area increment, and thus changes to the height-diameter relation can be predicted. As regards any error propagation from growth modules included in *PrognAus*, which are fit to data from the Austrian NFI, no clear answer can be given for the latest formulation with the updated basal area increment function as of the time of writing. An earlier setup of *PrognAus* showed evidence of both cancellation and continued propagation of errors from the independently developed models (Vospernik et al., 2010).

Because this type of modelling addresses a representation of individual trees under several different climate scenarios, the computer intensive simulation lends itself poorly for studies aiming to provide wall-to-wall forecasts. Thus, we chose to generalise the modelling results with a static reduced model, as described in the next section.

2.2. The GAMM formulation and feature variables

For the static reduced model, we used the stand-level growth ratio as the response variable. As the *gross volume production* includes both standing live volume as well as losses due to mortality, the stand-level growth ratio (*GR*) is always positive,

$$GR_l = \frac{Gross\ Volume\ Increment_l}{Gross\ Volume_{l-1}} \tag{1}$$

where the gross volume is produced in a stand until the end of a period given by the index. The time steps used were single years. We expect *GR* to take a right-skewed distribution of real positives as when the carrying capacity of live volume on a site is approached, either due to environmental constraints or with respect to the maximum packing density of the trees, the denominator (gross volume production up until the period) becomes increasingly large compared to the numerator (growth volume during the period), and the resultant *GR* becomes small.

We considered growth as being the product of factors pertaining to site, species, stand and climate, (Newnham, 1964, Kahn, 1994). We thus represent the climatic variables of interest as a modifier of the potential growth, the state of which is then dependent only on site, species and stand characteristics. Consequently, we model our data with a log link and a gamma distribution ($\Gamma(\cdot)$), implying that the additive components have a multiplicative effect on the untransformed target variable and ensuring that it is always a real positive.

In general terms, a *GAM* can be expressed as

$$g(E(Y)) = \alpha + \sum_{i=1}^{p} f_i(X_i), \tag{2}$$

where the mean of the target variable, transformed through the link function *g*, is a sum of an intercept, α, and *p* smooth functions. In our case, we used a log-link. Each of the *p* smooth functions f_i is a sum of *k* simpler, fixed basis functions (b_{ij}), in our case *thin-plate regression splines*; these can be expressed as

$$f_i(x) = \sum_{j=1}^{k} \beta_{ij} \bullet b_{ij}(x) \tag{3}$$

where the β_{ij} – terms need to be estimated.

To account for the hierarchical nature of the data, random effects were introduced to the model. The final *GAMM* formulation was:

$$ln\left(\mathrm{E}\left(\mathrm{GR_{mlq}}\right)\right) = \mathbf{Z_{mq}b} + \beta_{m0} + \mathrm{f_{m1}}\left(\boldsymbol{\beta}_{m1}, \mathbf{X}_{mlq1}\right) + \mathrm{f_{m2}}\left(\boldsymbol{\beta}_{m2}, \mathbf{X}_{ql}\right)$$

$$\boldsymbol{X}_{mlq1} = \left\{Volume_{mlq}, Age_{mlq}\right\}, \boldsymbol{X}_{ql} = \left\{Prec_{ql}, Prec_{ql-1}, Temp_{ql}, Temp_{ql-1}\right\}$$

$$\boldsymbol{b} \sim \mathcal{N}(0, \psi)$$

$$GR_{mlq} \sim \boldsymbol{\Gamma}\left(E\left(GR_{mlq}\right), \phi\right) \tag{4}$$

In (4), *l* is the index of the growth year, *m* the species mixture, *q* a triplet block location, *Prec* is the total precipitation during the year (*mm* m^{-2}), and *Temp* is short for the mean monthly mean temperature (°C).

The terms f_{m1} & f_{m2} are species mixture-specific tensors, a type of smooth which allows for anisotropic relations between covariates (such as when they are on different scales). The first tensor expresses the dependency of *GR* on stand state variables (gross production at the beginning of the growth year *l* and age during the growth year *l*). The second expresses the interactions between the climatic growth conditions of the growth year *l* and the preceding year *l-1*. Due to the flexible tensor structure, we did not transform these variables to represent climatic indices (details of the climatic variables are given in section 2.4).

Finally, the remainder of the *GR* not attributable to the parametric species-wise intercepts, β_{m0}, interactions between gross volume and age, or climatic factors represent the variation in *GR* as the result of differing inherent site productivities among the simulated stands – which can reasonably be considered as a random gaussian variable: our random effect. Note that the ***Zb*** random intercepts are at the level of each individual stand.

2.3. Model fitting

The *GAMM* was fit by *mgcv* [v. 1.9–0] by means of *fast REML* smoothness selection (Wood, 2011). The number of basis functions was increased until saturation. Regarding the choice of the number of basis functions, see Appendix A.1. Goodness of fit was assessed as the proportion of the null deviance explained by the model, which was 93.8 %. A plot of predicted versus observed values is shown in Fig. A3-1.

Smooth functions of several additional environmental variables were fit to the residuals of our final model, to assess if inclusion of additional variables could improve the model. In all cases, the deviance explained was below 5 %.

Of the parametric coefficients (intercepts), only the coefficient for *P. sylvestris*-stands was significantly ($p < 0.05$) different from the base intercept, corresponding to a base growth rate of 75 % of that of *Q.* spp. The random effects tasked with controlling the hierarchical structure of the data were found to be non-normal, as assessed from the QQ-plot (not shown in article), although this departure from normality would probably be of limited importance, c.f. Simpson (2024).

In conclusion, the model evaluations showed that the estimated *GAMM* provided an appropriate generalisation of the *IBM* results (Fig. 2) for all the stand types. However, *Q.* spp. stands showed some notable outliers exceeding 3 standard deviations, although on average the predictions aligned with the results from the *IBM* model. All predictions were carried out for stands where the random effect was assumed to be null. This is not to be confused with the marginal model, which for our model would be dependent on the variance of the random-effects and thus would be inappropriate with respect to our joint random-effect formulation.

2.4. Climatic scenarios

To predict growth on a pan-European scale, we retrieved precipitation rate (kg m^{-2} s^{-1}), minimum and maximum daily near-surface air temperature (*tasmin, tasmax*) (K) from downscaled monthly climatologies at 30 arc-seconds spatial resolution developed for the *CMIP5* project, e.g. Taylor et al. (2012), for four of the compared general circulation models (*GCM's*). These were ACCESS1.3 (*Australian Community Climate and Earth-System Simulator,* Bi et al., 2013), CMCC-CM (*Centro Euro-Mediterraneo sui Cambiamenti Climatici Climate model,* Scoccimarro et al., 2011), MIROC5 (*Model for Interdisciplinary Research on Climate*

version 5, Watanabe et al., 2010) & CESM1-BGC (*Community Earth System Model version 1.0 with Biogeochemistry,* Lindsay et al., 2014). The simulations retrieved were: *Historical, RCP 4.5* and *RCP 8.5*. The climatologies (Karger et al., 2019, 2020) were downloaded from chelsa-climate.org. Points for further processing were selected from the global datasets based on the geographic criteria [−13 < *longitude* < 30 and 35 < *latitude* < 65]. Grid cells falling outside country borders as delineated by the Natural Earth Admin 0 dataset (v. 5.11, boundary lakes not included) were removed. Points falling inside the British Isles were removed at the authors discretion, as data underpinning the *GAMM* only included locations in mainland Europe.

2.4.1. Data processing & feature engineering

Pre-processing required calculating an annual proxy variable for temperature: the mean monthly mean temperature (*mean temperature*), i.e. the arithmetic mean of the mean of the monthly mean maximum and minimum near-surface air temperatures (A4). Similarly, monthly precipitation rates were aggregated to annual precipitation (*mm / m^2*).

To harmonise the length of simulations, the period 1922–2005 was selected for the historical scenario whilst the period 2017–2100 was used for the two forecast scenarios (*RCP 4.5, RCP 8.5*) with changing climatic conditions. Since information of the previous growth year is required, note that the simulation length is 82 years (1923–2005; 2018–2100).

For each cell in the climatic grid, the simple mean of the climatic variables from the *GCM's* for each year was taken as input to iteratively calculate the gross volume production at the end of the next period for each stand type using the developed *GAMM*. To ensure comparability between the species types while considering the different ecological life-history traits as expressed in terms of a more rapid or conservative accruement of biomass, the initial age of the evaluated predictions was set to 60 years (above the lower quartile for all inventoried stands), and the initial *gross volume production* set to mean live standing volume per hectare of each stand type.

2.4.2. Handling extrapolation

To limit extrapolation, every prediction from a development series of the iterative procedure was required to be within a given distance from the nearest data point simulated with the *PrognAus IBM*. Since data become very sparse in high dimensions, we modified a procedure (*mgcv::exclude.too.far*) [v. 1.9–0] by Simon Wood (2011) to exclude grid points for prediction which are situated >0.1 in Euclidian distance from the nearest data point on the unit plane (min-max scaling) from any two interacting climatic covariates (A5).

In total, the number of potential grid points in the area of interest was 222′785. Of these, 219′770 points were within the limits set to avoid extrapolation (98.6 %). In total, this left 164.2 M data observations (219′770 grid points * 3 climatic scenarios * 3 stand types * 83 simulated years).

2.5. Time-series development

Since Europe encompasses a relatively wide range of climates, we identified regions predicted to undergo similar growth trajectories to simplify interpretation of results by decision-makers in assessing regional trends over time.

For each grid point, predicted *gross volume production* of the different combinations of climate experiments and species, was then considered to constitute a record constituting 82 rows (years) by 3 (species) * 3 (climatic scenarios) columns.

To identify similar regions projected to develop similarly, the grid points were clustered to minimise the within-group sum of squares by the k-means algorithm AS 136 (Hartigan and Wong, 1979) as implemented in '*stats::kmeans*'. The tested number of clusters was 1–15; the scree-plot is shown in the appendix (fig. A.6). The final number of clusters chosen was 5 – grid point cluster attribution is shown in the results (Fig. 9).

For interpretable output, graphic summaries from these clusters were retrieved in terms of:

1. Smoothed development of the gross volume production per scenario and species (see appendix fig. A.7).
2. Species-wise climatic tensor term contribution to the linear predictor (linear combination of the predictive terms) from the *cluster-average mean temperature* and *annual precipitation* as well as their corresponding values from the previous growth year, Figs. 8–12.
3. Smoothed development of the gross volume production per scenario and species relative to the historical species-wise development, Fig. 13.

Note that the response of the tensor term *cluster average* climatic variables will not correspond exactly to the tensor term *response average* of the individual raster cells.

2.6. Impact assessment of GCM scenario variability

To assess the impact of between model scenario variability to gross volume production as assessed by our model, we took the following approach: note that in eq. (4), the tensor regulating the climatic response, $f_{m2}(\boldsymbol{\beta}_{m2}, \boldsymbol{X}_{ql})$, can be evaluated independently of all other terms for a given climatic scenario and species-mixture. It represents the average climatic response in our dataset for a given year combination. In any scenario, a higher cumulative climatic response (sum) indicates more favourable conditions for total volume production.

We assume that this response sum for a given scenario and species-mixture is normally distributed between GCM's.

$$S_{qmsg} = \sum_{l \in sg} f_{m2}\left(\beta_{m2}, X_{qlsg}\right)$$

$$S_{qmsg} \sim \mathcal{N}\left(\mu, \sigma^2\right)$$

Where *S* is the sum of the evaluation of the climatic tensor *f2* for species-mixture *m* across all years, *l,* given annual climatic variables *X* for a site *q* under scenario *s* by model *g*.

As outlined in section *2.4.2*, we again retain only model, scenario climatologies with all values within a given distance of the nearest data-point from the scenarios the triplet sites were exposed to during simulation with *PrognAus*. The number of available models *G* can thus vary between 0 and 4.

We then for grid-point calculate the mixture-wise mean scenario response sum $\mu_{S_{qms}}$, and, if possible, its corrected sample standard deviation $\sigma_{S_{qms}}$.

$$\mu_{S_{qms}} = \frac{\sum_{g \in s} S_{qmsg}}{|g|}$$

$$\sigma_{S_{qms}} = \sqrt{\frac{1}{|G| - 1} \sum_{g \in G} \left(S_{qms}^{(g)} - \mu_{S_{qms}}\right)^2}$$

We are then interested in the probability that the true mean ratio *R* of the response sum $\mu_{S_{qms}}$ for a given mixture, location and compared scenario (s_1: *Historical*, s_2: *RCP 4.5* or *RCP 8.5*) is greater than (more favourable for gross volume production) 1 or <1 (less favourable for gross volume production). Note that these two probabilities are complements, and the statement is equivalent to $P\left(\mu_{S_{qms_2}} - \mu_{S_{qms_1}} > 0\right)$.

We define the difference of the means $\mu_D = \mu_{S_{qms_2}} - \mu_{S_{qms_1}}$ and its standard deviation as $\sigma_D = \sqrt{\sigma^2_{\mu_{S_{qms_2}}} + \sigma^2_{\mu_{S_{qms_1}}} - 2\rho\sigma_{S_{qms_1}}\sigma_{S_{qms_2}}}$, where ρ is the sample Pearson correlation coefficient. The standardized difference is then $Z = \frac{\mu_D}{\sigma_D}$.

Since *Z* follows a standard normal distribution, the probability that

the difference is positive is $P\left(\mu_{S_{qms_2}} - \mu_{S_{qms_1}} > 0\right) = \Phi(Z)$. Where $\Phi(Z)$ is the cumulative distribution function of the standard normal distribution.

3. Results

In the following, we first present results in terms of gross total production, i.e. aggregated growth across the projection period for different parts of Europe. Second, we compare *gross volume production* and associate uncertainty stemming from inter-model (GCM) variability for the different climate scenarios with that of the reference scenario. Third, we present the clustering into regions and present the developments in each of these.

In Fig. 3, the *gross volume production* at the end of the simulation period is presented for the three scenarios. In Fig. 4, comparison with the historical scenario is made in relative terms.

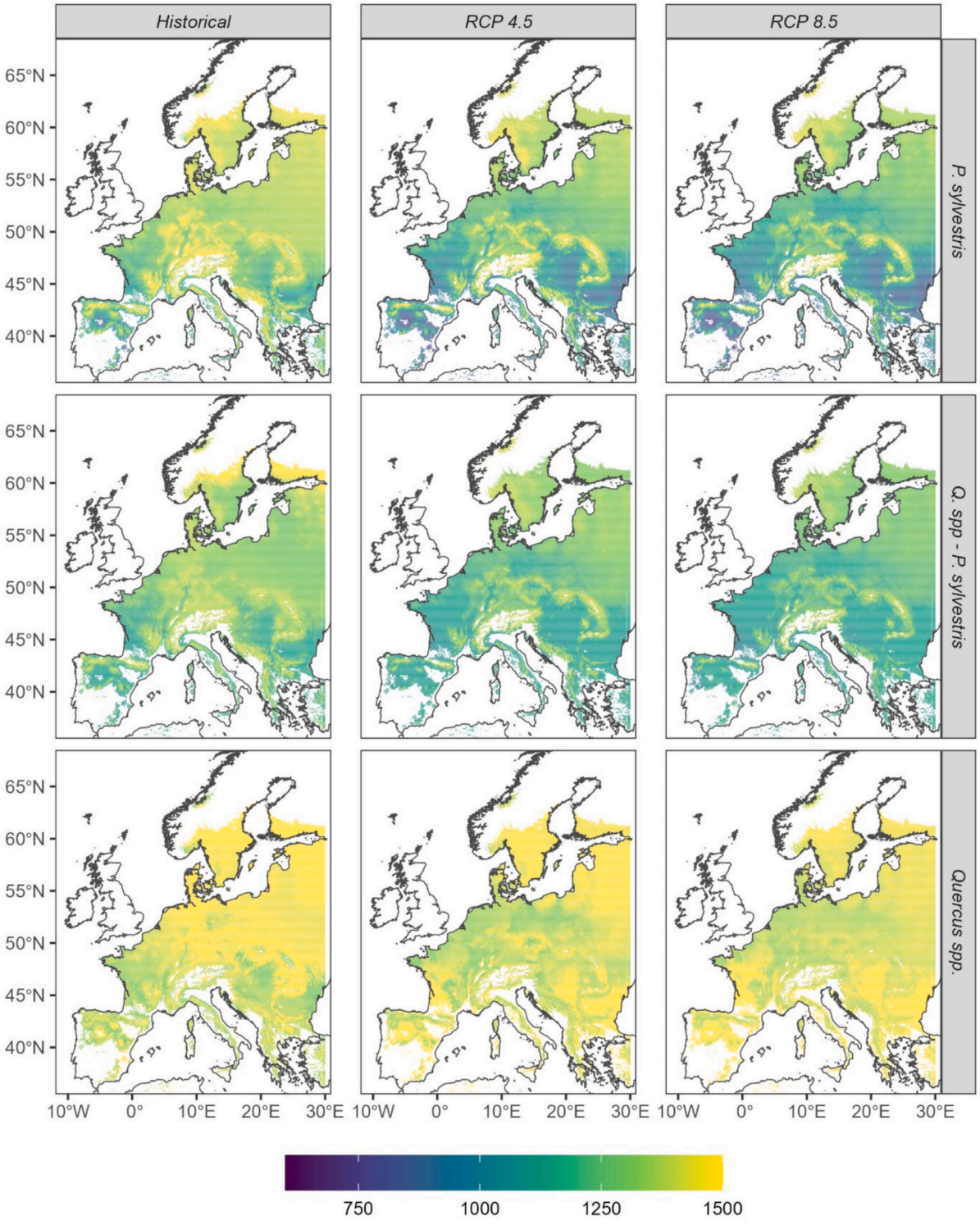

Fig. 3. Gross volume production at the end of the simulation period (m^3 ha^{-1}). Growth in response to scenario-wise yearly mean climate variables across included GCMs.

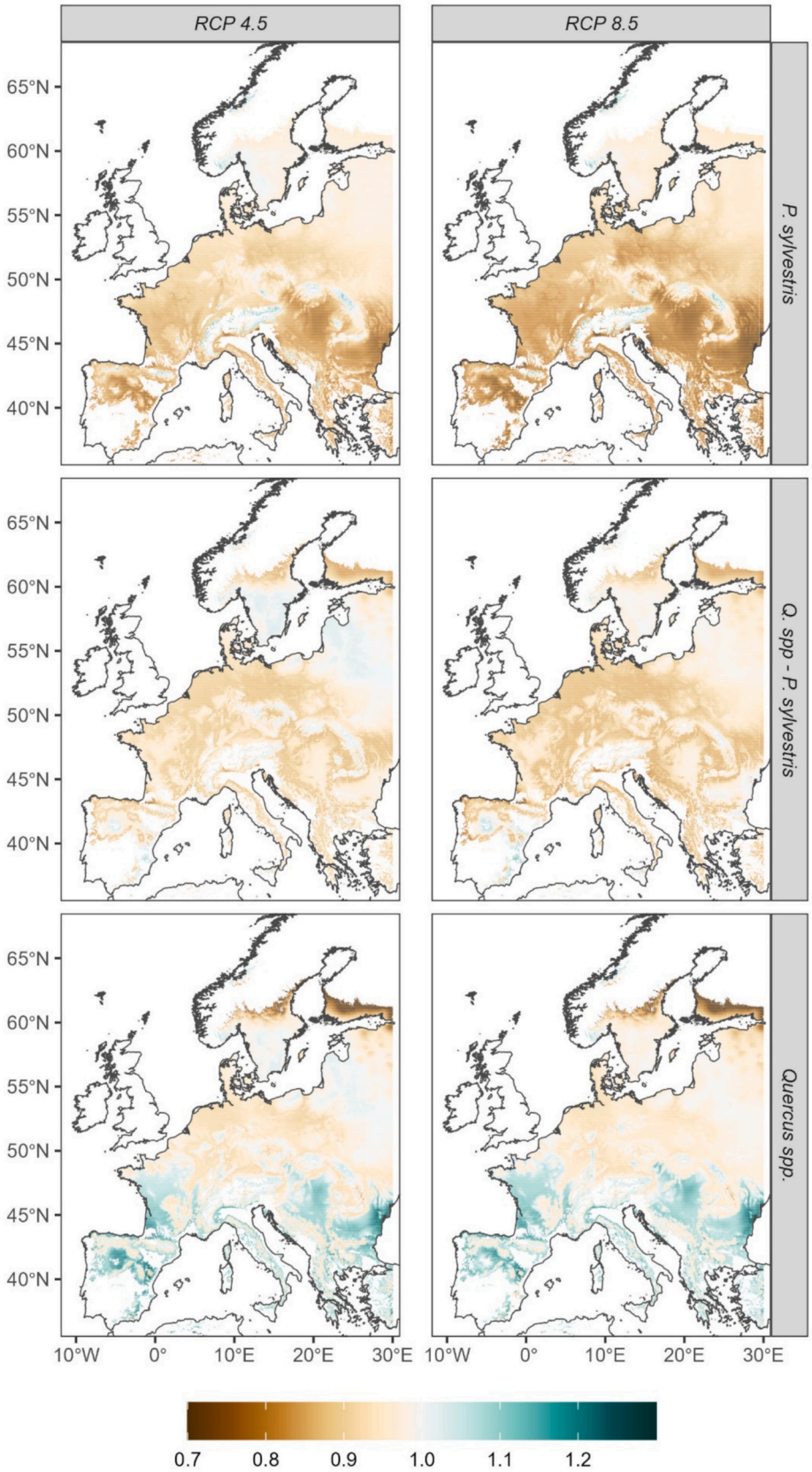

Fig. 4. Gross volume production at end of the simulation period expressed as a proportion of the gross volume production at the end of the historical scenario. Growth in response to scenario-wise yearly mean climate variables across included GCMs.

The areas of highest gross production for *P. sylvestris* for the historical scenario were predominantly located in central and northern Europe (Fig. 3). A particularly productive zone was apparent on either side of the middle and upper Rhine valley, and in the foothills of the large European mountain ranges. Substantial reduction of these areas appeared already under the *RCP 4.5* scenario, and this reduction was accentuated under the *RCP 8.5* scenario (Fig. 4). Particularly areas in southern France, the Pannonian basin, the Wallachian plain and Danube delta demonstrated severe reductions in total production relative to the historical scenario. Interestingly, the lowlands of these same areas showed increases (5–10 %) for *Q.* spp. under the *RCP 4.5* experiment, which were generally maintained also during the *RCP 8.5* scenario. Projections for the Netherlands, Belgium, northern France, Luxembourg, Germany, Poland, and the Czech Republic showed a widespread decline (5 to 15 %) across stand types (Fig. 4).

Rather than comparing the potential development of any single stand, we show (Fig. 5), the ratio of the mean climatic response sums across the included *GCM's*. This disregards in such respect the timing at which any individual stand from our data may be at its peak level of gross volume production. Note the greater extent of the map coverage, as we are no longer filtering the time-series to at least maintain a maximum distance from each tensor, but only the climatic response tensor. It becomes apparent that the mean climatic response, taken over the entire scenario, indicates a general increase in productivity across the southern Nordics and Baltic states for all species-mixtures, and that, this is a development with strong agreement between the models (Fig. 6). However, as can be seen in Fig. 6, the Swedish and Finnish areas north of 60th parallel are reflected in increasingly few models, and in some cases only in a single model, for which no uncertainty between the GCM's could be computed (grey color).

For *P. sylvestris* dominated mixtures in continental north-western Europe and on the northern European plain we see the largest area of signed change between the *RCP 4.5* and *RCP 8.5* scenarios, where a weak positive trend under *RCP 4.5* to the historical scenario changes sign when the more severe *RCP 8.5* scenario is compared.

Meanwhile, stands of the *Q.* spp. species-mixture show a widespread, positive improvement in the climatic response sum across the future scenarios (Fig. 5), with strong agreement between the included models (Fig. 6). Note again the exception north of the 60th parallel, where there is scarce coverage from the climatology the triplets underlying our SRM were simulated under.

The disparity between Fig. 4, the ratio of the gross volume production of a stand during the *GCM* model average climatology during future scenarios (*RCP 4.5, RCP 8.5*) compared to the historical, and Fig. 5, the ratio of the mean climatic response sum across *GCMs* during future scenarios compared to the historical, could reasonably point at the importance for the result of matching the stage of growth, i.e. gross volume-age tensor of eq. (4), with periods of more suitable weather.

3.1. Cluster results

The grid clusters were challenging to group by any contemporary bioclimatic zone, owing to large changes in climate, and we therefore introduced group-names specific to this study. These were (Fig. 7): 1) Boreal, 2) Continental, 3) Hemiboreal-Orotemperate, 4) Franco-Pannonian, and 5) Mediterranean.

Inspecting the clusters further (Figs. 6–10), we can observe that there is a very large variation around trends in total annual precipitation. The largest differences in the climatic response (multiplicative climatic modulator extracted from linear predictor) seem thus to be associated with periods of change in the mean monthly temperature, which will be explored further in the sections *3.1.1–3.2* below.

Note that we here denote changes in absolute terms as the *percentage point (p.p.)* change, since we have a reference level of 1 (100 %) for the mean response of the climatic modulator across the data material. It was thus considered to be more easily compared to the figures than the percentual change. For example, in the Boreal cluster, Fig. 8, a decline from a modulator term value of about 1.4 during the 1920s to 1.05 in 2100 would be referred to as a loss of 35 percentage points (1.4–1.05), rather than a 25 % decline, which does not relate as clearly to the figures displaying the value of the modulator.

3.1.1. Boreal cluster

The Boreal cluster (Fig. 8) displays small differences between the climate modifier of the stand types during future scenarios but indicate that there has been a particularly advantageous historical period relative to the species climatic baselines up until the millennium shift. *Q.* spp. and mixed stands of *Q.* spp.-*P. sylvestris* responded particularly positively to periods of colder weather (below ~4.5 °C). *P. sylvestris* stands are slowly responding less positively to the annual weather as temperature increases.

3.1.2. Continental cluster

Continental sites (Fig. 9) show extremely similar climatic responses between the species compared to their respective climatic baselines. A slight positive response compared to baseline (c. 5 %) is maintained during the entire historical scenario and up until around 2030, but drops thereafter as temperatures rise above c. 11 °C. Under the *RCP 4.5* scenario, temperatures then vary around 12 °C and all species perform at c. 95 % of the climatic baseline, whilst under the *RCP 8.5* scenario temperatures continue to increase to almost 14 °C. A large differentiation among the stand types then ensues, where *P. sylvestris* demonstrates a rapid decline of about 20 p.p. between 2050 and 2100. The productivity of mixed stands of *Q.* spp.-*P. sylvestris* declines some 5 p.p. during the same timeframe, whilst *Q.* spp. manages to turn the negative trend and again perform above the climatic baseline after c. 2075.

3.1.3. Hemiboreal – Orotemperate cluster

Among the Hemiboreal-Orotemperate pixels (Fig. 10), the stand types maintain particularly distinct climatic responses (*P. sylvestris* > *Q.* spp. – *P. sylvestris* > *Q.* spp.) up until c. 2040, when a loss of c. 5 p.p. for *P. sylvestris* and mixed stands of *Q.* spp.-*P. sylvestris* begin to be incurred up until 2100. *Q.* spp. is slightly less affected, c. 2.5 p.p. This begins around the time that temperatures rise above 9 °C. Whilst temperature rise mellows out at c. 10 °C in the *RCP 4.5* scenario, during the *RCP 8.5* scenario it continues to rise to 12.5 °C, up from c. 7 °C largely maintained during the historical period. This entailed larger losses, all species finally performing at around 90–95 % of climatic baseline year 2100. *P. sylvestris* stands stand out, dropping upwards of 20 p.p. between 2030 and 2100.

3.1.4. Franco-Pannonian cluster

The Franco-Pannonian cluster showed a strong differentiation in the climatic responses between the stand types (Fig. 11). Between 2000 and 2050 there was an almost linear increase in the climatic modifier for *Q.* spp. of about 10 percentage points (p.p.) from 0.95 to 1.05. A slightly stronger reaction for the *RCP 8.5* scenario than for *RCP 4.5* was observed. Meanwhile, mixed stands of *Q.* spp.-*P. sylvestris* demonstrated a decline in their climate modifier response of c. 5 p.p. between 1990 and the 2010's. Declines were observed for *P. sylvestris* in both scenarios, from about 0.95 to 0.8 between 1990 and 2050, as mean monthly mean temperatures increase from about 11 °C to 14 °C. Further temperature increases, towards 17 °C under the *RCP 8.5* scenario, result in a dramatic loss of a further 20 p.p. between 2050 and 2100.

3.1.5. Mediterranean cluster

Stands in the Mediterranean cluster demonstrate distinct differences between stand types with respect to their climatic reactions (Fig. 12). Whereas mixed stands of *Q.* spp.-*P. sylvestris* are largely nonresponsive to the mean climatic changes, maintaining a productivity of around 90 % of baseline, *Q.* spp. stands react positively to simulated changes – incurring an increase in the climate modifier up until c. 2050. For the

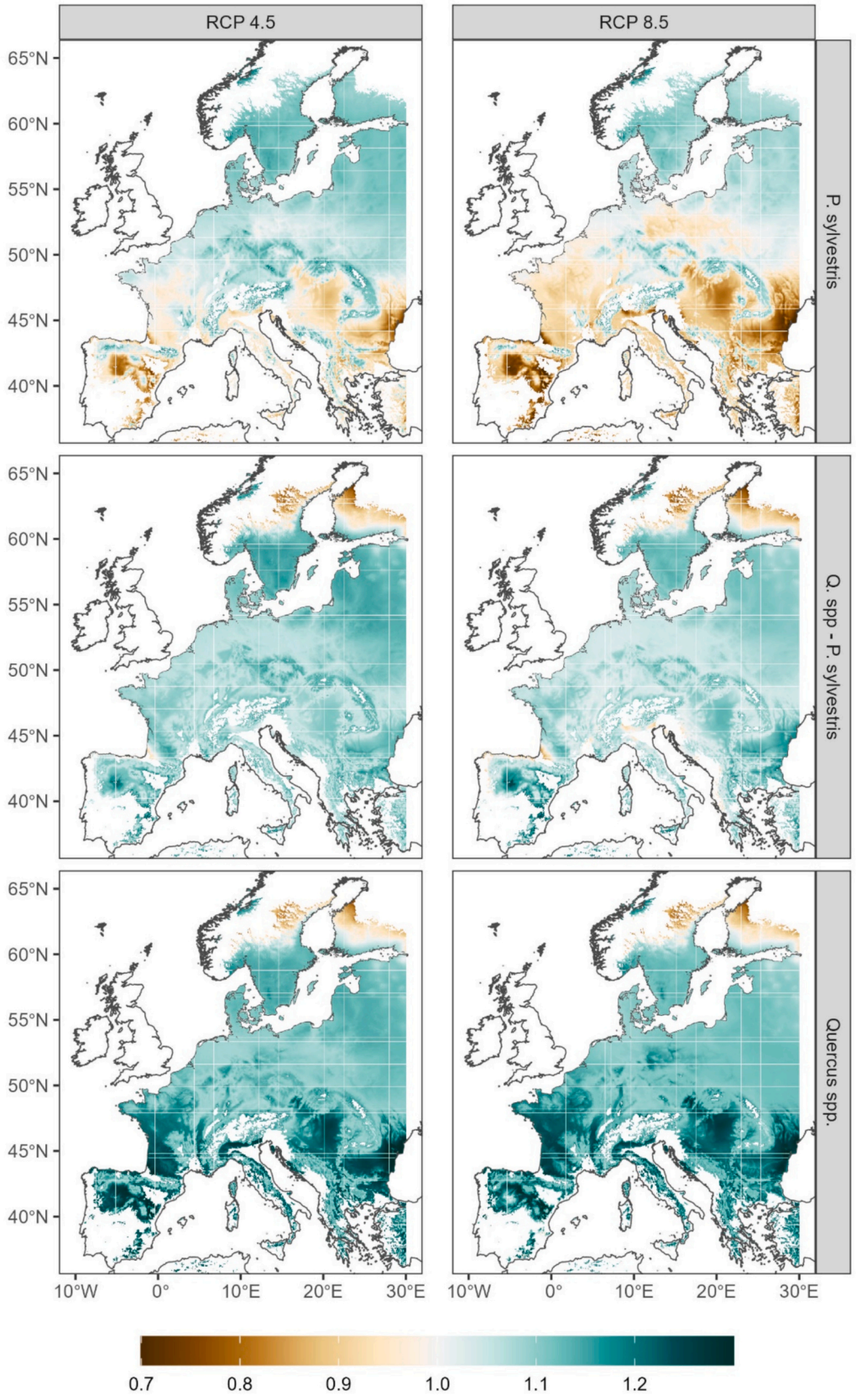

Fig. 5. Quotient of Mean climatic response sums across GCMs of future scenario (RCP 4.5, RCP 8.5) against historical scenario.

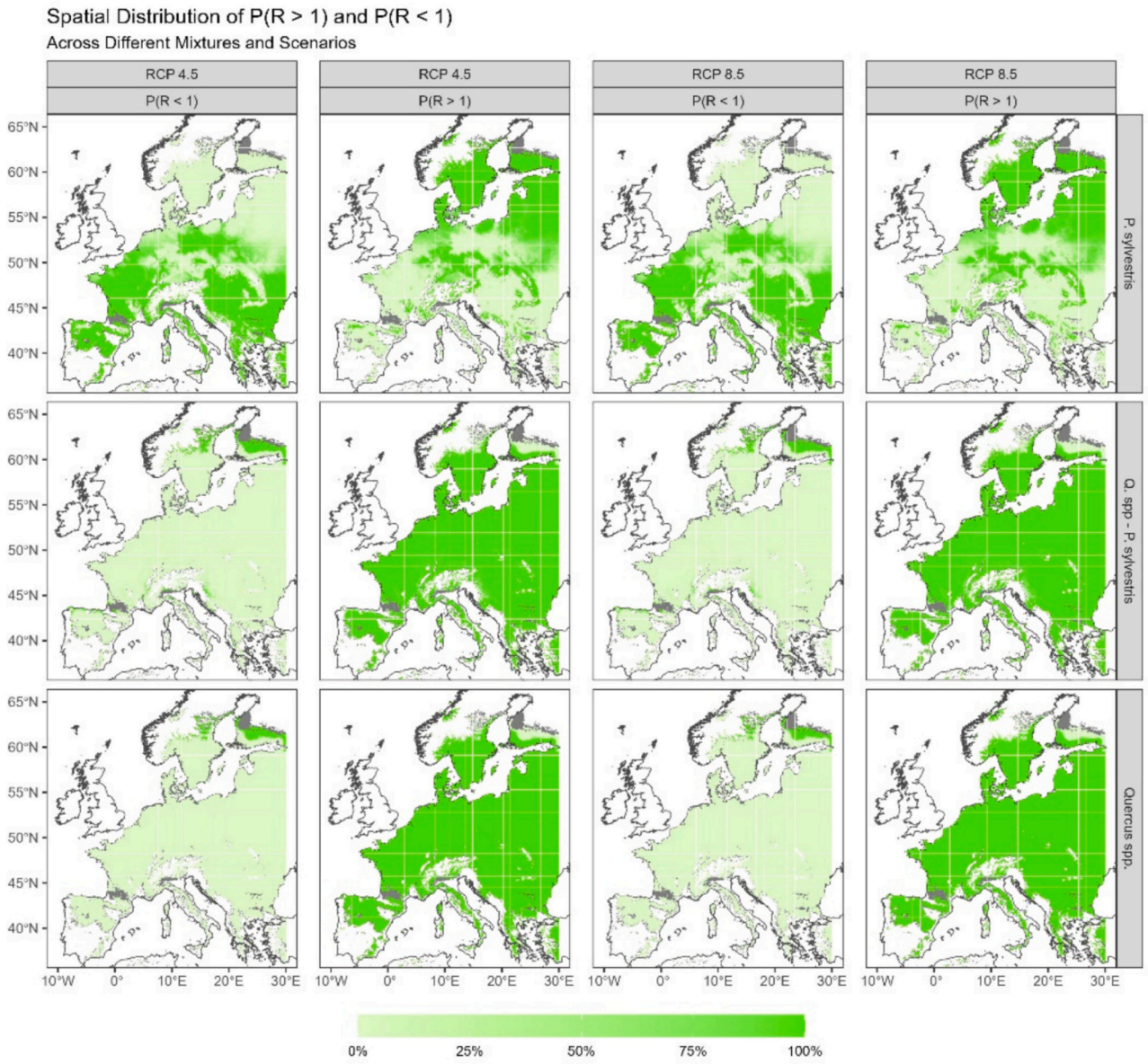

Fig. 6. Probability (0–100 %) of climatic response sum of future scenario (columns) exceeding, or becoming less suitable, than the historical scenario, by species-mixture (rows). Marked in grey are areas with only scenarios from a single GCM within a suitable distance from the climatologies which the triplet sites were exposed to during simulation. For full resolution, the reader is referred to the electronic print of this article.

RCP 8.5 scenario, there is a rapid decline in the modifier response when the temperature exceeds 16 °C, amounting to 35 p.p. (from 1.1 to 0.75). *P. sylvestris* stands begin to decline from a maintained climate response of about 0.85 from the 1980s down to 0.6 around 2060 under both future scenarios. Under the *RCP 8.5* scenario, where temperatures continue increasing beyond 15 °C, there is a further decline down to a climatic modifier response of 0.5 at 2060.

3.2. Relative differences between climatic scenarios

In terms of the total production incurred at a given stand age (Fig. 13, relative; figure of absolute development available in appendix, Fig. A8), the particularly advantageous climatic situation for the Boreal cluster under the historical scenario rapidly incurs a heavy relative debt on *Q.* spp. and mixed stands of *Q.* spp.-*P. sylvestris*. However, there is little differentiation between the two future scenarios relative to the historical. *Q.* spp. manages to achieve some 77.5 % of its total production of the historical scenario at 2100, whilst the mixed stands of *Q.* spp.-*P. sylvestris* are somewhat more competitive, maintaining 87.5 %.

In the Continental and Hemiboreal-Orotemperate clusters the distance between the stand types' *gross volume production* remains roughly the same during the simulated periods. At the same time, there is a change of order between the stand types as *P. sylvestris* experiences more severe declines both due to life-history trade-offs (Fig. A8), but also due to compounding losses from the climatic response term relative to the historical scenario. Close inspection of facets 2, 3 in Fig. A8 indicate that for both the Continental and Hemiboreal-Orotemperate clusters, *Q.* spp. was expected to surpass the total production of *P. sylvestris* at stand ages of 110–120 years during the historical scenario. The stand age at which this occurs is lowered under the two future scenarios by c. 5 years.

During the future scenarios (*RCP 4.5, RCP 8.5*), Boreal *Q.* spp. stands come to surpass *P. sylvestris* much later (c. 25 years; facet 1, Fig. A8), most likely due to the loss of the, for *Q.* spp., conducive climate during the historical period. In contrast, much like in the Continental and Hemiboreal-Orotemperate clusters, Franco-Pannonian and Mediterranean *Q.* spp. stands surpass the total production of their *P. sylvestris* counterparts some 20 (*FP*) to 10 (*Med*) years earlier.

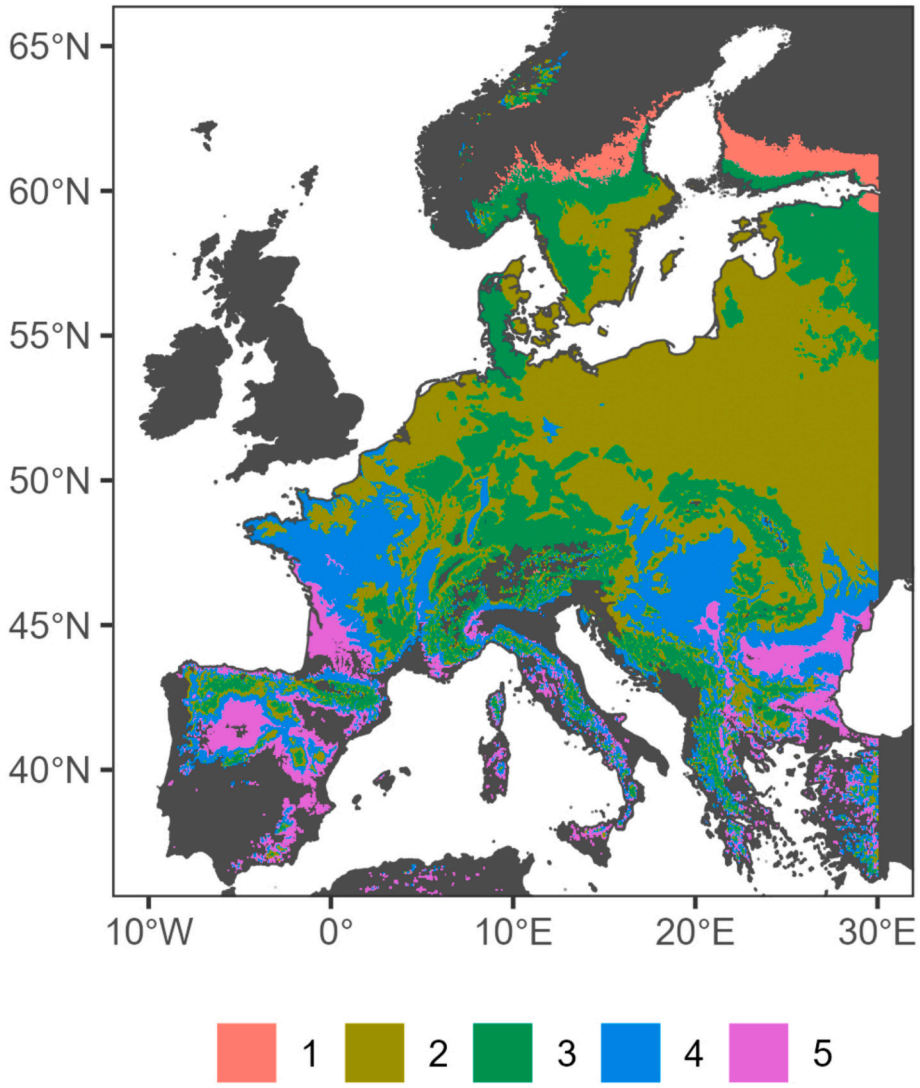

Fig. 7. Cluster attribution of grid points: 1) Boreal, 2) Continental, 3) Hemiboreal-Orotemperate, 4) Franco-Pannonian, and 5) Mediterranean. Dark background for areas with climatic conditions too far from training data.

4. Discussion

In this study, we present detailed spatially explicit forecasts of the future growth of *P. sylvestris* and *Q.* spp. across large parts of Europe. This was achieved by training a climate-sensitive static reduced model on the detailed tree- and stand level results from individual sites. Growth declines were foreseen for *P. sylvestris* for all studied parts of Europe, larger in the south than in the north. For *Q.* spp., the patterns were more complicated, with growth increases in several parts of central and southern Europe, demonstrating the importance of spatially explicit modelling beyond simple longitudinal and latitudinal interpolation. This type of results has a potential to guide local and regional level forest management in adapting to climate change, e.g. species selection when thinning or planting.

In making the results from Vospernik et al. (2024) spatially explicit we had several options. One option was to interpolate based on geographical proximity and other covariates, but given the location of the study sites, such interpolation would consider a relatively small region and imply a poor use of the information. A stand- or cohort-level aggregation viz. (Cao, 2014; Ekö, 1985; García, 2017) accounting for the greater-than-the-sum-of-parts emergent nature of mixtures could be applied to the problem – but we considered it would be inappropriate to publish an interim set of differential equations before we have acceptable climate-sensitive mortality models, as a result of the risk for misplaced implementation. Therefore, developing a climate-sensitive static reduced model was considered the most appropriate alternative. In doing so, we evaluated whether to fit specific models to each mixture category, but evaluations indicated that no notable improvement in the goodness of fit of the models was obtained (the deviance was found to be 98.9 % of that of the compound model). Further details are given in the appendix, e.g. related to simulated residuals pertaining to the gamma distribution and differences of variances between groups. Note that to facilitate replicability of our results, precipitation rates for predictions were *not* modified for realism as described in preceding papers (Vospernik et al., 2023, 2024). We suggest that future studies involving empirical forest models could benefit from developing API's (application programming interfaces) to substantially reduce labour associated with forecasting sites – potential gains for development of SRM's would involve the ability to run initial stands at many different locations, and thus better represent the complex model (reduction of potential bias, variance) which could stem from unequal representation of continuous covariates.

In the following, we first contrast our findings with those of Vospernik et al. (2024), before comparing our results with other previous studies.

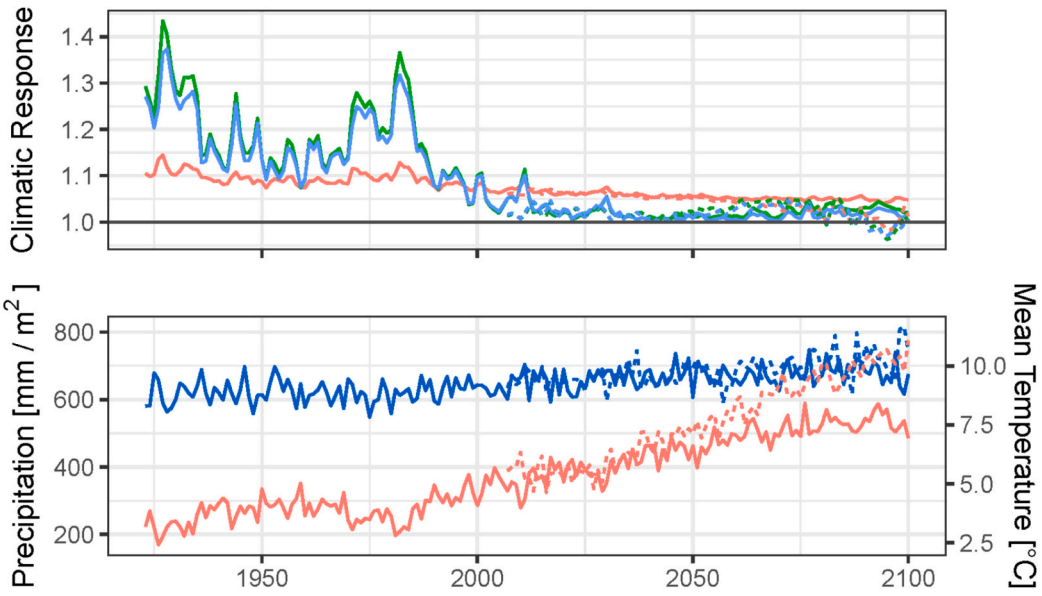

Fig. 8. Boreal cluster. Upper panel: Climatic response term corresponding to the lower panel. *P. sylvestris* (red), Q-P (green), Quercus spp. (blue). Lower panel: smoothed means of the clusters mean monthly mean temperature, red (°C) and total annual precipitation, blue (mm m^{-2}). Before 2006, single solid lines show the historical development. After 2006: the solid line depicts the RCP 4.5 scenario and the dashed line the RCP 8.5 scenario.

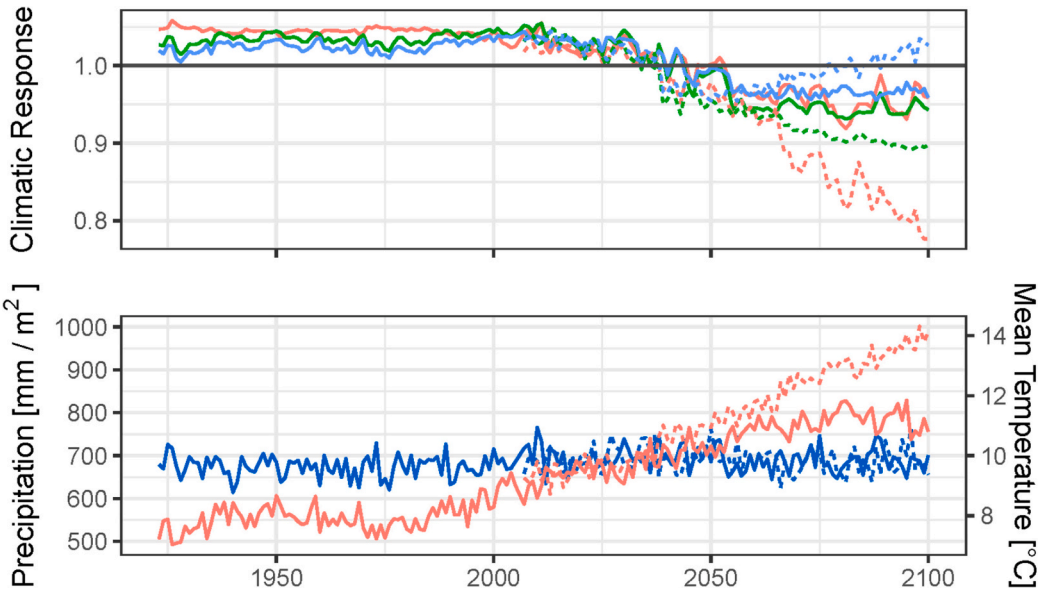

Fig. 9. Continental cluster. Upper facet: Climatic response term corresponding to the lower facet. *P. sylvestris* (red), Q-P (green), Quercus spp. (blue). Lower facet: smoothed means of the clusters mean monthly mean temperature, red (°C) and total annual precipitation, blue (mm m^{-2}). Before 2006, single solid lines show the historical development. After 2006: the solid line depicts the RCP 4.5 experiment and the dashed line the RCP 8.5 experiment.

4.1. *Comparison with Vospernik et al. (2024)*

Compared to Vospernik et al. (2024), our findings demonstrate more clearly the importance of the geographic locale. Whilst both longitude and latitude were highly significant predictors in Vospernik et al. (ibid.), the linearity of the terms placed strong limitations on the fidelity of the linear mixed model. The cluster-wise reductions in *gross volume production* at the end of the simulation period in response to the average climate from this study are of the same magnitude as the expected reductions at corresponding latitudes reported in Vospernik et al. (ibid.) and reinforces that in the Mediterranean and Franco-Pannonian regions, strong reductions were simulated for *P. sylvestris*, but more tempered reductions are observed also for the *P. sylvestris* – *Q.* spp. stand mixture. However, in this study the Mediterranean and Franco-Pannonian regions show a notably higher gross volume production of *Q.* spp. stands under future climate experiments (*RCP 4.5, RCP 8.5*) than under the historical scenario. Likewise, in terms of the total gross volume production, *Q.* spp. remains competitive with *P. sylvestris* in Boreal and Hemiboreal-Orotemperate clusters at higher ages. Relative to the historical scenario, future climate experiments yield responses in total volume production, which are quite similar but entail slightly more severe reductions for *P. sylvestris* in *RCP 8.5* compared to in the *RCP 4.5* scenario. *Q.* spp. and *P. sylvestris* – *Q.* spp. stand types show very similar responses during the future scenarios, but in contrast to Vospernik et al. (2024), *Q.* spp. does show increases in total volume production relative to the historical scenario in the Franco-Pannonian and Mediterranean clusters.

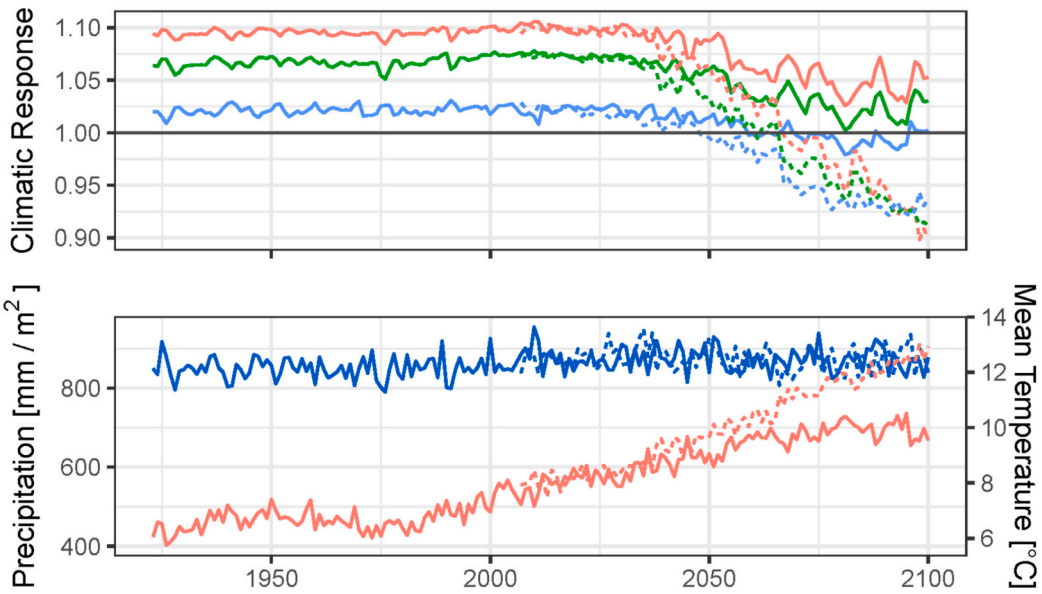

Fig. 10. Hemiboreal-Orotemperate cluster. Upper facet: Climatic response term corresponding to the lower facet. *P. sylvestris* (red), Q-P (green), Quercus spp. (blue). Lower facet: smoothed means of the clusters mean monthly mean temperature, red (°C) and total annual precipitation, blue (mm m^{-2}). Before 2006, single solid lines show the historical development. After 2006: the solid line depicts the RCP 4.5 experiment and the dashed line the RCP 8.5 experiment.

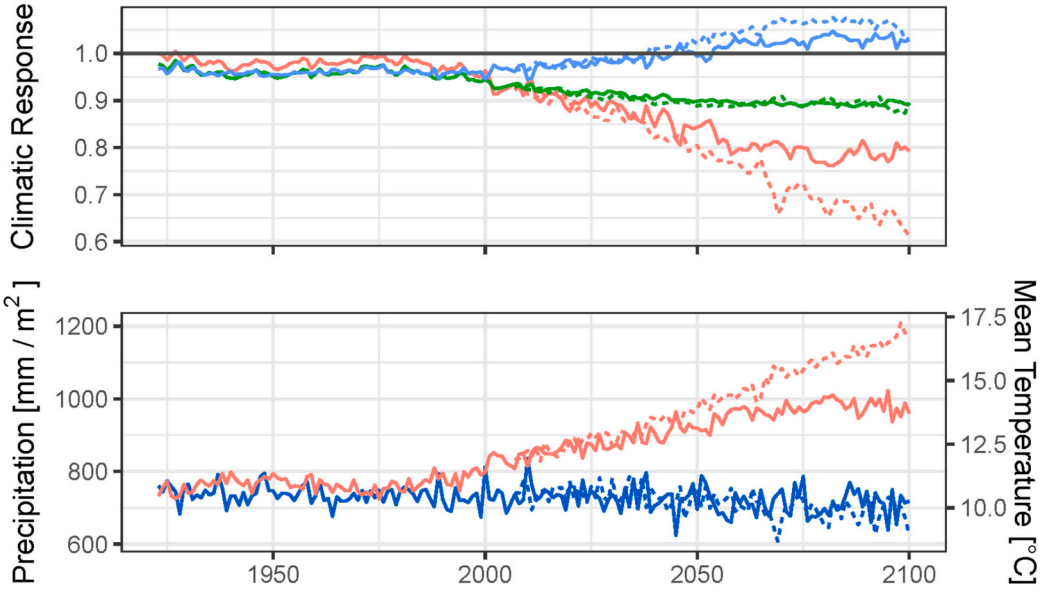

Fig. 11. Franco-Pannonian cluster. Upper facet: Climatic response term corresponding to the lower facet. *P. sylvestris* (red), Q-P (green), Quercus spp. (blue). Lower facet: smoothed means of the clusters mean monthly mean temperature, red (°C) and total annual precipitation, blue (mm m^{-2}). Before 2006, single solid lines show the historical development. After 2006: the solid line depicts the RCP 4.5 experiment and the dashed line the RCP 8.5 experiment.

4.2. Comparison of results to regional studies

4.2.1. Nordics

Kellomäki et al. (2008) simulated the development of Finnish NFI permanent sample plots by linking environmental modifiers from a physiological model to predict tree growth. Given a business-as-usual management regime for the years 1990–2099 with the *SRES A4* emission scenario, implying rises of atm. CO_2 concentrations from 352 ppm to 841 ppm. The results showed considerable increases of stocking levels (86 %) towards the end of the period compared to current stocking levels in northern Finland. For southern Finland, no major changes were identified in terms of stocking. The growth ($m^3ha^{-1}\ yr^{-1}$) increased in northern Finland from 2.2 to 4.6 $m^3ha^{-1}\ yr^{-1}$ (109 %), while in southern Finland the increase was only 12 %. Species-wise results were not presented, but *P. sylvestris* was described to increase its growth throughout the entire country, although less so in south-western and south-eastern

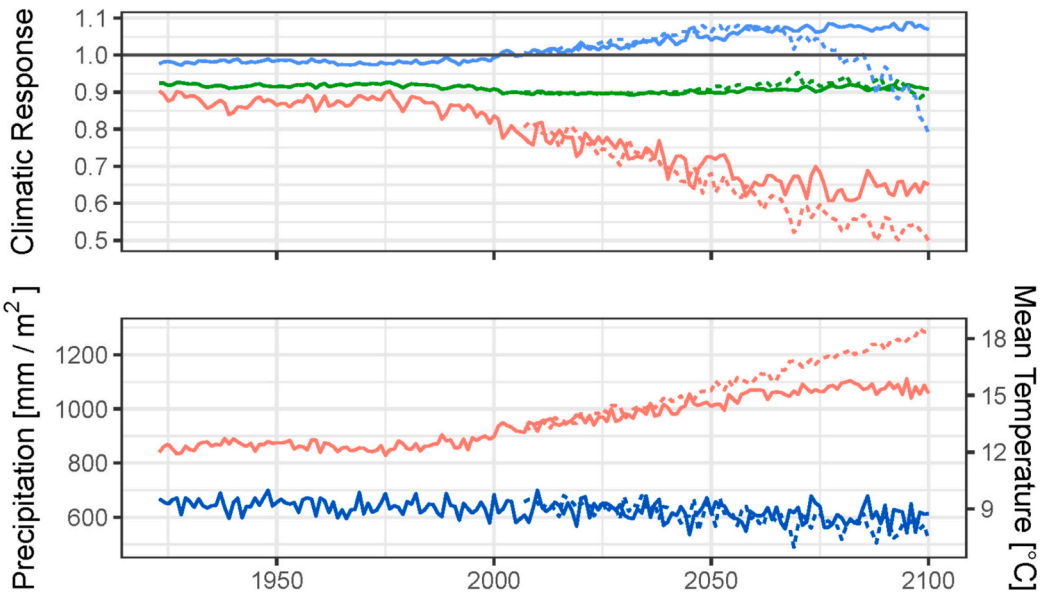

Fig. 12. Mediterranean cluster. Upper facet: Climatic response term corresponding to the lower facet. *P. sylvestris* (red), Q-P (green), Quercus spp. (blue). Lower facet: smoothed means of the clusters mean monthly mean temperature, red (°C) and total annual precipitation, blue (mm m^{-2}). Before 2006, single solid lines show the historical development. After 2006: the solid line depicts the RCP 4.5 experiment and the dashed line the RCP 8.5 experiment.

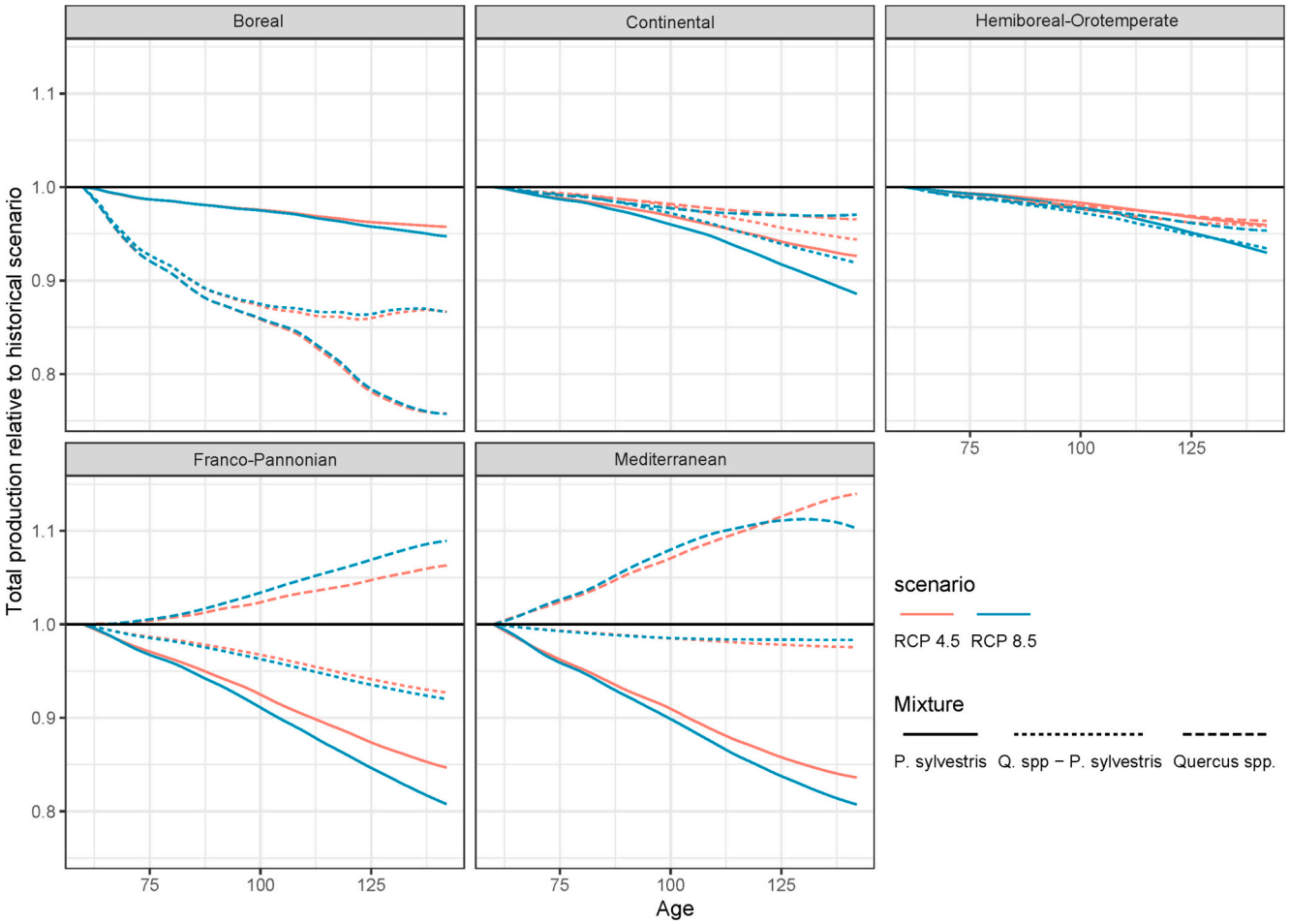

Fig. 13. Total gross volume production by cluster and stand type during the RCP 4.5 & RCP 8.5 scenarios relative to the historical scenario (smoothed).

parts due to drought. Similar results were reported by Kellomäki et al. (2018), Kellomäki and Väisänen, 1997), and Briceño-Elizondo et al. (2006). In our study, growth of *P. sylvestris* did not increase in southern Finland, suggesting that underlying soil types may not be as responsive as, i.e. fresh till sites, or that such differences may occur due to differences in temporal resolution of the chosen climatic scenarios. However, in alignment with our results, a study by Mäkinen et al. (2017) found that apart from the most recent years, no major changes in the site index of *P. sylvestris* during the last 50 years in southern and central Finland were identified. Site index is the expected height of the 100 stems with the thickest diameter per hectare at a reference age, and very strongly correlated with gross production capacity, explaining 80–90 % of variation in the rotation maximum mean annual increment cf. (Mensah et al., 2022).

In alignment with the results from Goude et al. (2022), we find limited impact on the growth of *P. sylvestris* in the parts of southern Sweden which were included in our study. However, we found slightly larger effects for the *RCP 8.5* simulation, where the reduction amounted to up to 10 % along the south-eastern Swedish coastline (Fig. 4).

In particular, we note the evidently advantageous climatic conditions for *Q.* spp. inferred to have been present in southern Scandinavia during the previous century, coincident with colder periods (Fig. 8). This follows the northern boundary native distribution of *Q.* spp. (Eaton et al., 2016). We interpret this with some caution, as although it is within a stringent range criterion of our model, it may be outside the applicable range of the climate covered by the data underpinning the BAI-model and other routines in *PrognAus*. In any case, the distribution of temperate forest tree species is suggested to be restricted primarily by reproductive success, rather than survival (Morin et al., 2007) and growth. de Rigo et al. (2016) in Eaton et al. (ibid.) estimate the areas covered by the Boreal cluster to involve 'mid-low' to 'low' survivability. Comparing the response of the climatic smooth from our simulations for the Boreal Cluster to core samples from sample trees taken by the Swedish NFI dated to 1936–2005 (Diameter-weighted ring-width index (2010,2020)), we find a correlation coefficient of ~0.3 for *P. sylvestris* (60°N,62°N], and ~ 0.4 for *Q. robur* (all of Sweden), see appendix section A.9. This is promising, given that the BAI-model had an R^2 of 0.198 for *P. sylvestris*, and 0.459 for *Q.* spp. (Vospernik, 2021).

4.2.2. Continental Atlantic Europe

Vallet and Perot (2018) coupled transversal NFI data with longitudinal information from increment-cores by adopting a growth-potential modifier approach parametrised from the longitudinal information to adjust a basal area increment function from French NFI data. They found no significant mixture-effect of combining *P. sylvestris* and *Q. petraea*. Compared to the mean productivity 1950–2005, they found a slight (peak c. 5 %, Fig. 3 ibid.) increase under *RCP 4.5, 8.5* for *Q. petraea* around 2030, the gains of which were lost around 2060. For *P. sylvestris* the same peak appeared earlier in time in the *RCP 8.5* experiment but was much weaker for the *RCP 4.5* case. In contrast to *Q. petraea, P. sylvestris* continues to decline down to c. 95 % of the mean productivity 1950–2005 by 2100.

Whilst the trendline for Orléans forest, Fig. 3 in Vallet and Perot (2018) indicates a slight increase in productivity compared to 1950–2005 between c. 2000 and 2050, peaking at c. 5 % gain around 2025, our study shows that the climatic modifier in response to the mean climate in the Franco-Pannonian cluster is slightly stronger for *Q.* spp. than shown by Vallet & Perot (ibid.), and does not decrease towards 2100. *P. sylvestris*, on the other hand, demonstrates a much larger loss of productivity in our study. However, although based on the same climatic scenario, comparisons with our study are complicated given the large local variability within each group and potential differences in soil types.

Compared to results from the Netherlands, (Bouwman et al., 2021), we find that *Q.* spp. in the continental cluster is the least negatively affected of the 3 stand types under both climatic scenarios. Although the climatic scenarios utilised are not directly comparable, and Bouwman et al. (ibid.) instancing slightly younger (45 years) stands, we observe only minor reductions up until 2050, where *P. sylvestris* is slightly more affected (fig. 16). As can be seen in terms of the gross volume production (fig. 17), *P. sylvestris* is indeed the more productive species until c. 2060, although this is primarily because of the starting conditions.

4.2.3. Germany

Nölte et al. (2020) outfitted the 3-PG model, e.g. (Landsberg and Waring, 1997), with a leaf-phenology model to account for lengthened growing seasons. Without accounting for increases in atm. [CO_2], *RCP 4.5* and *RCP 8.5* provided an average + 2.7 % and + 3.8 % increase, respectively, in mean annual increment during the period 2020–2100 compared to the period 1935–2015 for stands of *Q. petraea* in south-western Germany. Further, Nölte et al. (ibid.) noted that variation within sites (for different climatic scenarios) was large and variation between sites was very large relative to the effect, highlighting the complexity of fairly representing change-at-scale in the presence of large variation between and within sites. Our results for the same area suggest a future of no change or mild decreases of 5–10 %.

4.2.4. Western Mediterranean

Our results for the development of stands of *P. sylvestris* in the western Mediterranean area indicate that reductions in productivity related to climatic change found by Pretzsch et al. (2023a) will continue under both of future climatic pathways evaluated (RCP 4.5, RCP 8.5). Furthermore, the decrease in climate vegetation productivity index (ibid.) 1975–2017 and the concomitant decrease in the productivity of unthinned stands of *P. sylvestris* is also present in our study, and of roughly comparable magnitude (loss amounting to ca. 10 p.p. in the climatic-response smoother between 1975 and 2015, Fig. 12).

4.3. Limitation of analysis

We have demonstrated how results from models of high complexity can be utilised for constructing a simpler static reduced model, at least to categories where the functional relationships to the investigated variables can be hypothesized to be maintained – and provide reasonable results, especially for generalising detailed results from individual study sites to larger regions.

The assumption of a maintained functional relationship within semantic species-groups can be expected to require considerable increases in model complexity for species more predisposed to local subspeciation. As shown by Kellomäki et al. (2018), categorical division of sites is practical for application and may thus continue to be implemented in future works, although ultimately will constrain a model within specific reaction norms (even if site-specific categories may come to change, e.g. floristic composition, depth to ground water, etc.). Simulations are thus constrained by the assumption of these holding constant.

As for the uncertainty about future conditions, notwithstanding the uncertainty inherent to the *GCMs*, we must bear in mind that due to the discrepancy between the temporal (month) and spatial (10's km^2)

resolution of the output, and the scale at which the effects experienced by plant populations are present (*days-weeks, local-regional*), the frequency and impact of extreme events may be inherently misrepresented (Lindner et al., 2014). More generally, the long-term mortality may be difficult to assess (Bugmann et al., 2019). Further, mortality is impacted by the species-mixture, cf. Pretzsch et al. (2023b).

We suggest that after the inclusion of climate-sensitive mortality routines, the effect of management interventions, e.g. thinning, could be evaluated regarding the potential to avoid undue mortality and identify *value* impact of climatic scenarios on combinations of species, site, and management, and that these evaluations include uncertainty stemming both from structural differences between stands, as well as variation within comparable climatic experiments by GCM's, e.g. (Gutsch et al., 2016; Nölte et al., 2020).

5. Conclusion

With a static reduced model (GAMM), we present the first application where an individual tree growth simulator has been applied to study potential growth at the subcontinental scale. Broad reductions of the growth of *P. sylvestris* stands across Europe were forecast, with reductions from inconducive climatic conditions throughout the Mediterranean and Franco-Pannonian regions already underway and expected to continue under both RCP 4.5 and RCP 8.5 scenarios. In the Hemiboreal-Orotemperate and Continental regions, the choice of climatic scenario holds sway over the development expected in the second half of the 21st century. Our results suggest the growth of *P. sylvestris* and *Q.* spp. in the southernmost regions of the present-day boreal biome, which has been widely expected to increase in productivity, may be limited by precipitation. Several localised regions across southern Europe suggested potential growth increases for *Q.* spp. compared to the historical reference period. Matching the growth pattern of the species-mixtures to temporal periods of potentially beneficial climates can have a notable effect on the outcome. Future studies looking at the potential productivity of tree species-mixtures are recommended to take such temporal effects into account.

CRediT authorship contribution statement

Carl Vigren: Writing – review & editing, Writing – original draft, Visualization, Methodology, Investigation, Formal analysis, Data curation, Conceptualization. **Sonja Vospernik:** Writing – review & editing, Writing – original draft, Supervision, Methodology, Data curation, Conceptualization. **Xavier Morin:** Writing – review & editing, Data curation, Conceptualization. **Maude Toïgo:** Writing – review & editing, Data curation, Conceptualization. **Kamil Bielak:** Writing – review & editing, Investigation. **Felipe Bravo:** Writing – review & editing, Conceptualization. **Michael Heym:** Writing – review & editing, Conceptualization. **Magnus Löf:** Writing – review & editing, Conceptualization. **Maciej Pach:** Writing – review & editing, Conceptualization. **Quentin Ponette:** Writing – review & editing, Conceptualization. **Hans Pretzsch:** Writing – review & editing, Conceptualization.

Declaration of competing interest

We have no declarations of competing interest.

Acknowledgements

The authors thank the European Union for funding the project "Mixed species forest management. Lowering risk, increasing resilience (REFORM)" under the framework of Sumforest ERA-NET. All contributors thank their national funding institutions to establish, measure and analyze data from the triplets. The Polish State Forests Enterprise also supported one of the Polish co-authors (Grant No: OR.271.3.15.2017). The Orléans site, OPTMix was installed thanks to ONF (National Forest Service, France), belongs to research infrastructure ANAEE-F; it is also included in the SOERE TEMPO, ZAL (LTSER Zone Atelier Loire) and the GIS oop network. FB is grateful for the support by the Spanish Ministerio de Ciencia e Innovación (# PID2021-126275OB-C21/C22) and by the Junta de Castilla y Leon, Spain, and the European Union for funding the Projects VA183P20 (SMART—Bosques mixtos: Selvicultura, Mitigacion, Adaptacion, Resiliencia y Trade-offs) and CLU-2019-01—iuFOR Institute Unit of Excellence of the University of Valladolid through the ERDF "Europe drives our growth". CV thanks the Knut & Alice Wallenberg Foundation for funding his PhD project.

The authors are grateful for the valuable comments provided by Profs. G. Ståhl and M. Ekström, as well as Dr. AA Mensah which have helped improve this paper.

Appendix A

A.1. On the assigned amount of basis functions

The number of basis functions is essentially arbitrary. As long as it can adequately model the underlying relation between the covariates and the dependent variable the exact amount is not important. The number of smooths included for the life-history tensor of each species was set to 8: resulting in a maximum possible degrees of freedom, k', of 8*8–1 = 63. The climatic response for each species was provided 5 functions per marginal smooth, i.e., k' = 5*5*5*5–1 = 624. Since for the fitted model, k' far exceeded the effective degrees of freedom for each tensor, we concluded the amount of basis functions provided is adequate, when interpreted in combination with the summary statistics (see results). Further increasing the number of basis dimensions would be a significant computational burden. The full rank of the model then appears as: 135 + 3*624 + 3*63 + 3 = 2199.

A.2. Observed versus predicted values

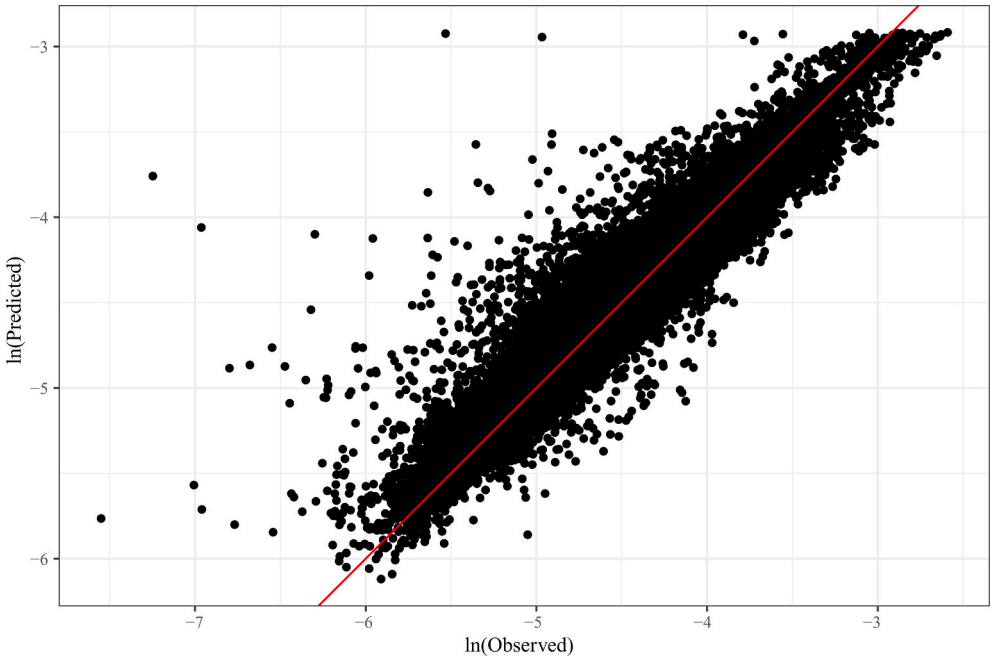

Fig. A2. Observed versus predicted GR values (ln-ln scale). The red line shows the 1:1 correspondence.

A.3. Further model diagnostics

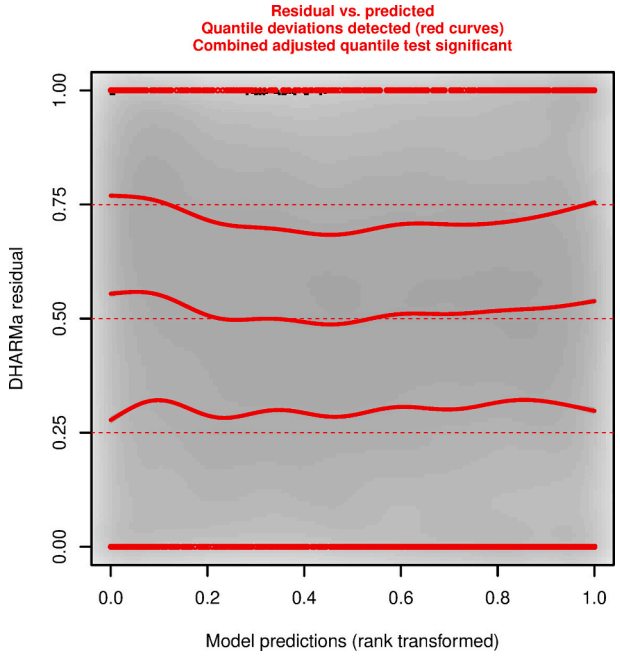

Fig. A3-1. Simulated residuals from the estimated Gamma distribution.

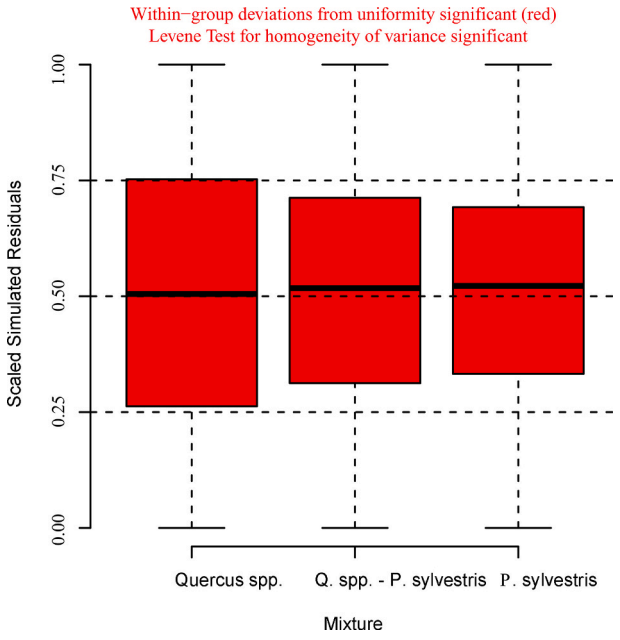

Fig. A3-2. Residual frequency versus expectation.

As can be observed in the diagnostic plots generated by *DHARMa* [v. 0.4.6] (Hartig, n.d.) (fig. A.3), the model appropriately fits the simulated responses. Quantiles of simulated Gamma residuals from the estimated distribution are close to the observed data (Fig. A3-1, left), albeit somewhat leptokurtic. This slightly increased variance stems at least partly from the lower deviance explained from the *Quercus* spp. group (Fig. A3-2., right).

A.4. On preprocessing of climatic data

Since said dataset is comprised of monthly values, the length of which from the technical specification is unclear, these were in accordance with Climate and Forecast Metadata Conventions assumed to hold a standard-length of 1/12 year, where a year in the standard (Gregorian) calendar is given as 365.2425 days. The time dimension was interpreted in the same way when expressed in terms of '*months since* …'.

A.5. Modified procedure for limiting extrapolation

Our modified procedure works as follows:

For each of our two sets of interactions (tensors), a plane is constructed from each unordered combination of covariates from results of the *PrognAus* IBM (our training data). This plane [0,1][0,1], contains all of the min-max normalised observations, scaled along their respective covariate axis between the minimum observation (0) and the maximum observation (1). Given a prediction point, which is not limited to [0,1], the Euclidian distance to the nearest observation in the training data must not exceed a distance of 0.1 (10 % of the range of the covariate, if the difference between the points were to lie along a single axis). Should this be true for any of the unordered combinations from either of the sets of interacting terms, the prediction point will be deemed to be too far from the underlying information, and the *entire* development series of which the prediction point is a part is discarded. Since the climatic data is shared among the plots simulated with the *PrognAus* IBM, and the climatologies from the GCM's are independent of the stand state – and known beforehand, we could exclude series containing climates too far from the training data before predictions were initiated for the series remaining. Age and total production were not known a-priori, since simulating the development of the stand by means of our developed GAMM is dependent on the previous states, and the observations of age and total production from the training data furthermore are specific to the different species. This is thus done in post.

A.6. Cluster scree-plot

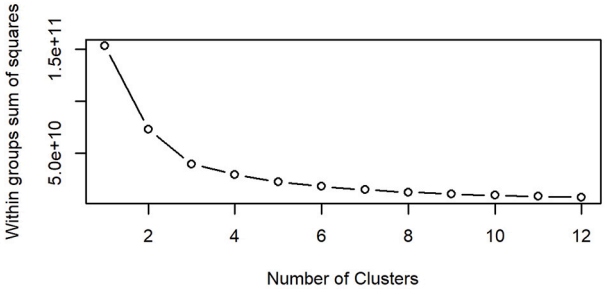

A.7. Behaviour of model tensors

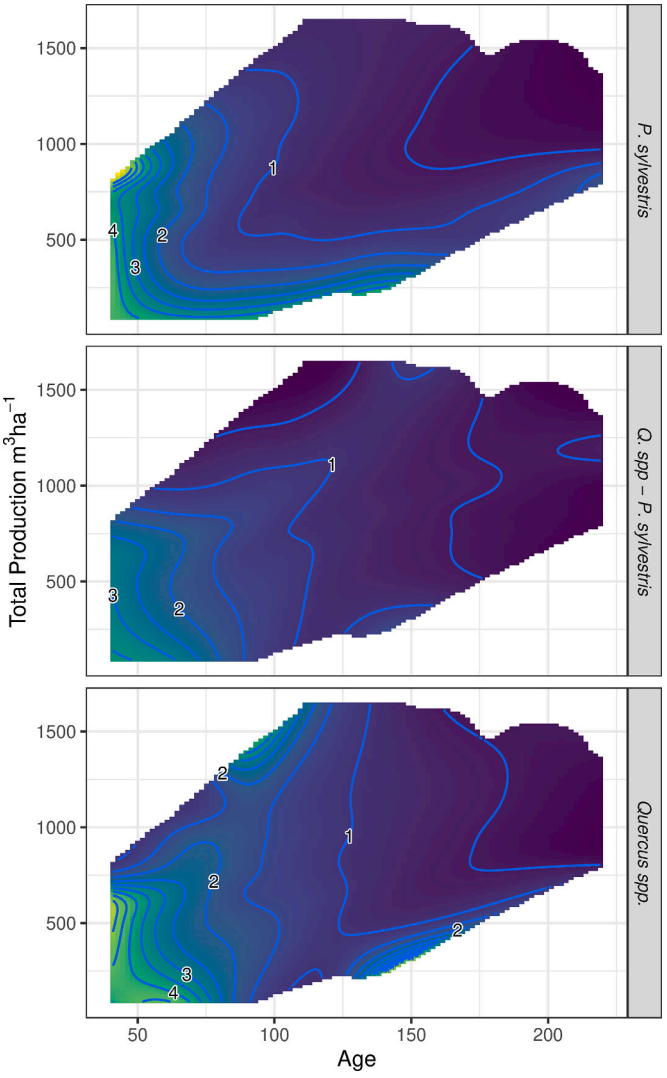

Fig. A7-1. Life-history tensor for each stand type. Base rate intercepts have been added to emphasize stand type differences. Contour lines connect states of equal output (GR, %). Coloured area indicates region within a distance of 0.1 on the scaled unit square of the covariates (gross volume production, age).

A.7.1. Gross volume production- age

Rapidly flattening inverse sigmoid slopes of growth rate (%) shown by the contour lines with increasing standing volume and age are typical for sigmoidal volume trajectories and is demonstrated by all stand types (Fig. A7-1). Slope of the contour lines indicate that *P. sylvestris* is somewhat more sensitive to *gross volume production* than the age of the stand, whereas *Q.* spp. stands show a more balanced response (equivalent limitation at young ages). *Q.* spp. stands show some rapid changes at particularly high or low volumes during intermediate to advanced ages, possibly indicating some overfitting.

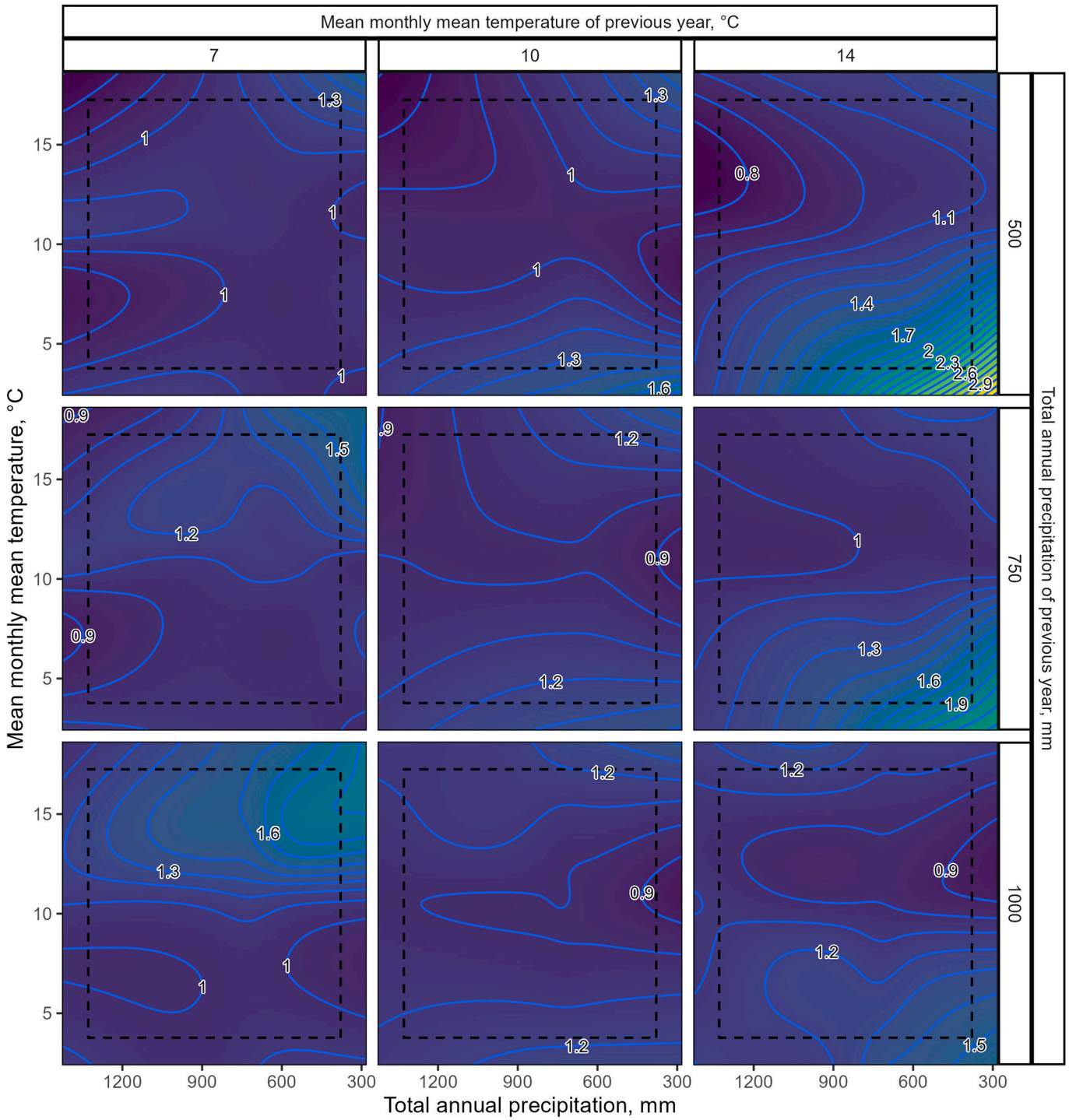

Fig. A7-2. Climatic smooth for the Q. spp. stand type – 4 terms. On abscissa: Total annual precipitation (mm). On ordinate: Mean monthly mean temperature (°C). Facets along abscissa and ordinate: subjectively chosen monthly mean temperature of previous year (°C) and total annual precipitation of previous year (mm), respectively. Contour-lines connect states of equal output.

A7.2. Climatic modifier

Faceting values will be referenced as follows in text: dry (500 mm), moderately dry (750 mm), wet (1000 mm); cold (7 °C), moderately warm (10 °C), hot (14 °C). As an example to aid the reader interpret the faceted plots over the response of the climatic smooths for the different stand types: To find the expected Growth rate of a given *Q.* spp. stand where the previous year was wet (1′000 mm total annual precipitation) and cold (Mean monthly mean temperature of 7 °C), and a growth year which has been moderately dry (750 mm) and quite hot (14 °C), inspect the left-bottom facet at the coordinates x = 750, y = 14 to obtain a *GR* of 1.4–1.5 (40–50 %) higher than the average climatic effect for a growth year.

Horizontal contour lines for *Q.* spp. climatic responses (Fig. A7-2) following moderate to hot indicate that *GR* is being primarily constrained by too high temperatures during the growth year. In contrast, particularly following a wet year, there is a large potential response to growth given a

combination of both high mean monthly mean temperatures and large amounts of annual total precipitation.

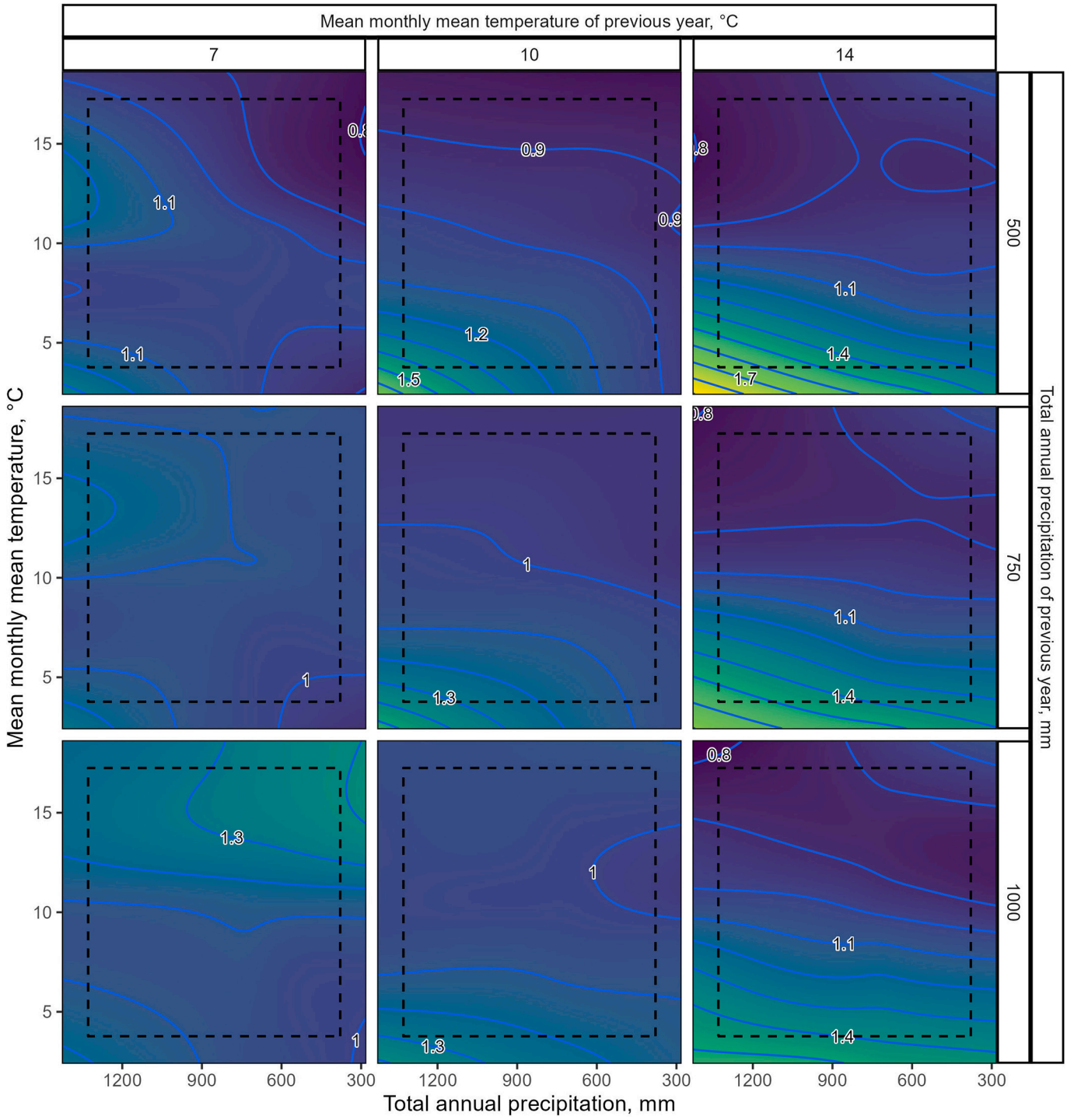

Fig. A7-3. Climatic smooth for the *Q. spp.* – *P. sylvestris* stand type – 4 terms. Layout as for fig. 15.

Much like *Q.* spp. (Fig. A7-2), the *GR* of the *Q. spp.* – *P. sylvestris* stand type (Fig. A7-3) shows a strong aversion to high temperatures following hot years. Following a moderately warm year, there is a stable preference for cool, wet years. After cold years (left facet), there is a positive reaction to higher temperatures, if the amount of precipitation supplied during the previous and current year are sufficient.

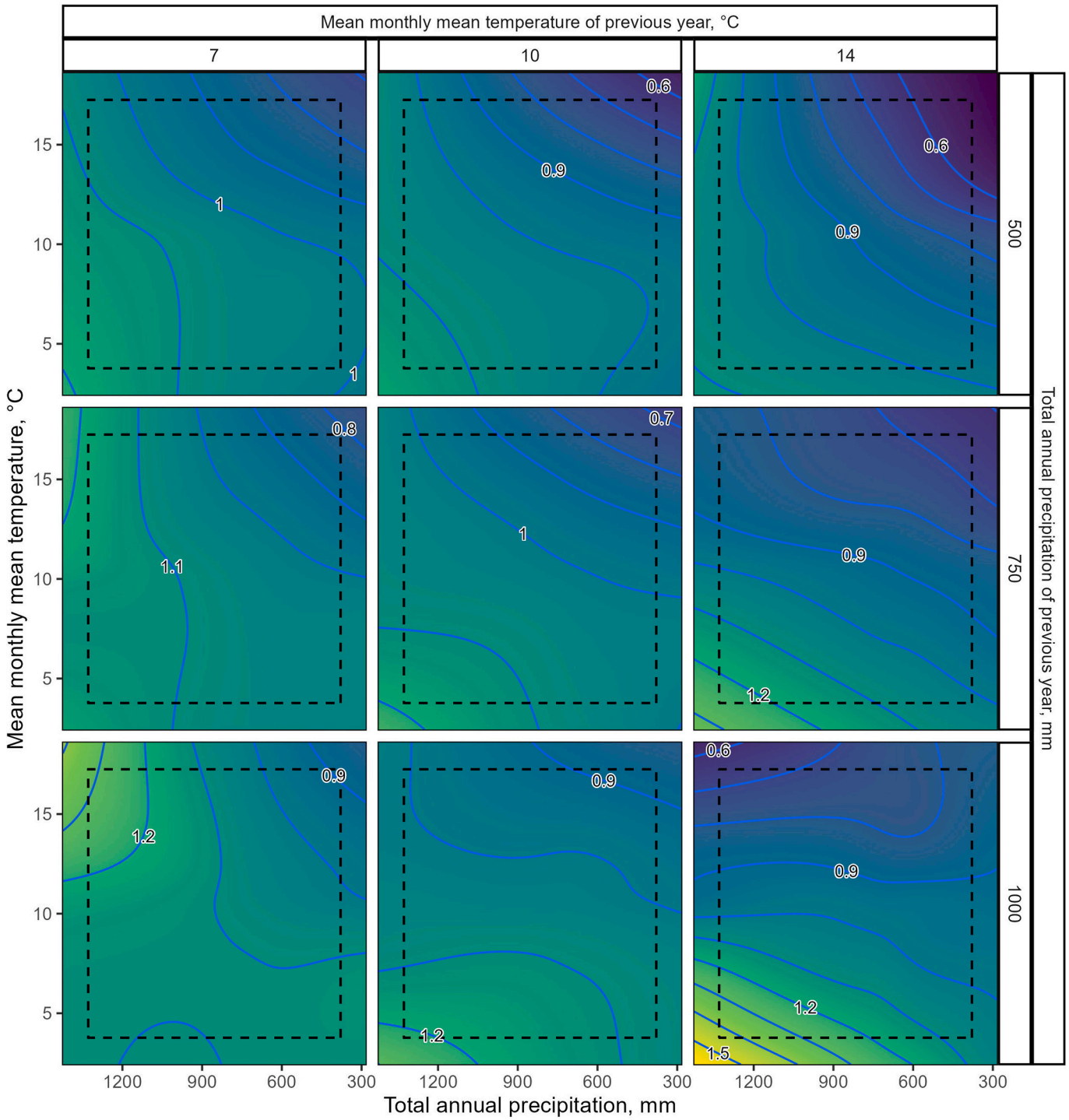

Fig. A7-4. Climatic smooth for the *P. sylvestris* stand type – 4 terms. Layout as for Fig. A7-2 and Fig. A7-3.

P. sylvestris (Fig. A7-4) clearly demonstrates *GR* being limited by both high mean monthly mean temperatures and low amounts of precipitation after a moderately warm to hot year. Growing years following cold years are only limited primarily by high temperatures, but across a wide range of the scale show strong responses to larger amounts of total annual precipitation. Following a wet and cold year there is even a positive response to a hot year, provided there is ample precipitation.

A.8. Absolute gross volume production development GAM smoothers

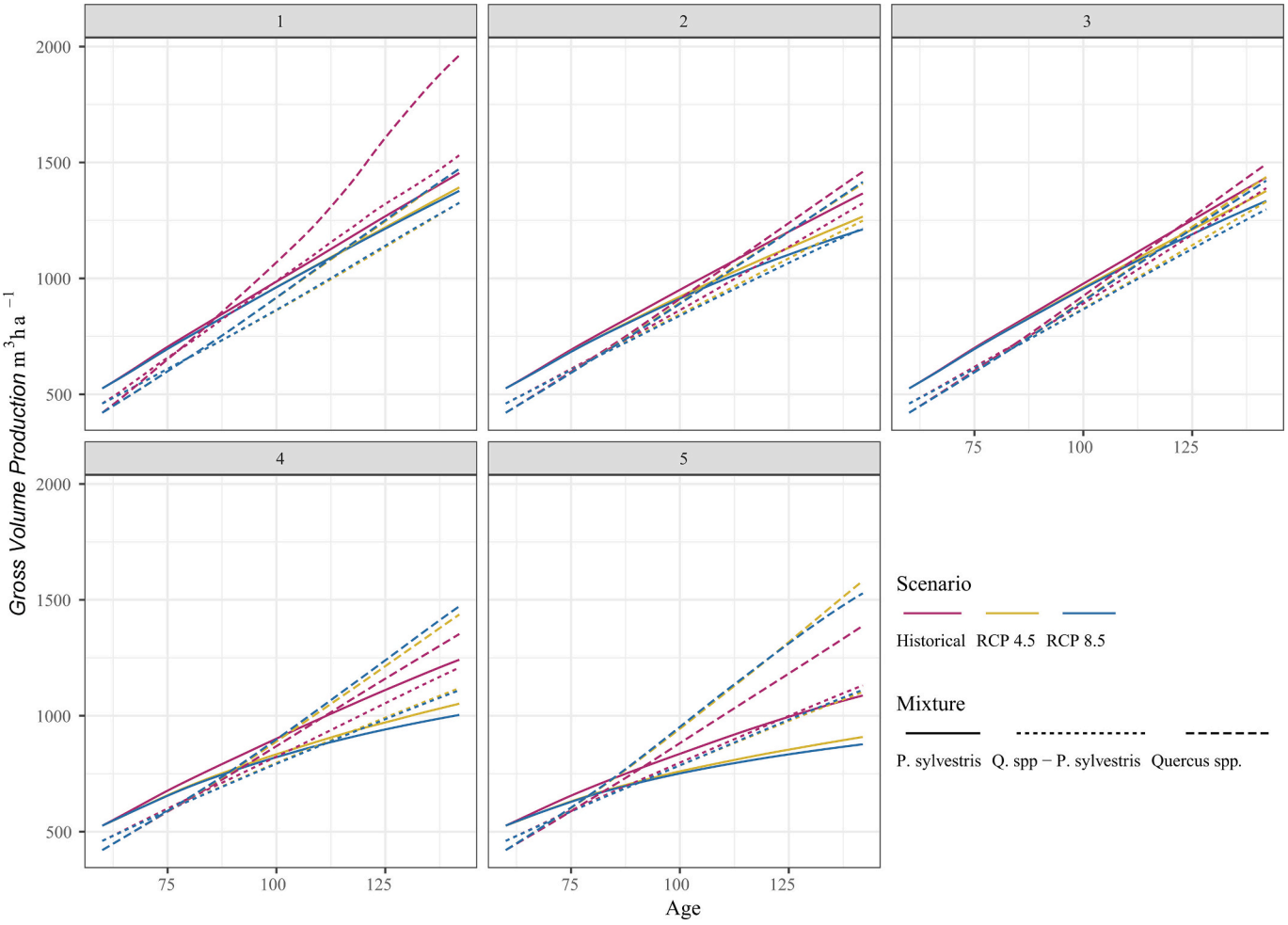

Fig. A8. GAM smoothers for absolute development of total production (gross volume production in cubic meters per hectare). Facets: 1) Boreal 2) Continental 3) Hemiboreal-Orotemperate 4) Franco-Pannonian 5) Mediterranean.

A.9. Swedish NFI Diameter-weighted Year-Ring Index, baseline (2010–2020) vs. Cluster 1 Simulation Results

NFI year-ring data from sample trees available from 1935.
In images: Solid dot, solid line: NFI year-ring index (baseline 2010–2020).
Triangle, dashed line: Cluster 1 climatic tensor response.

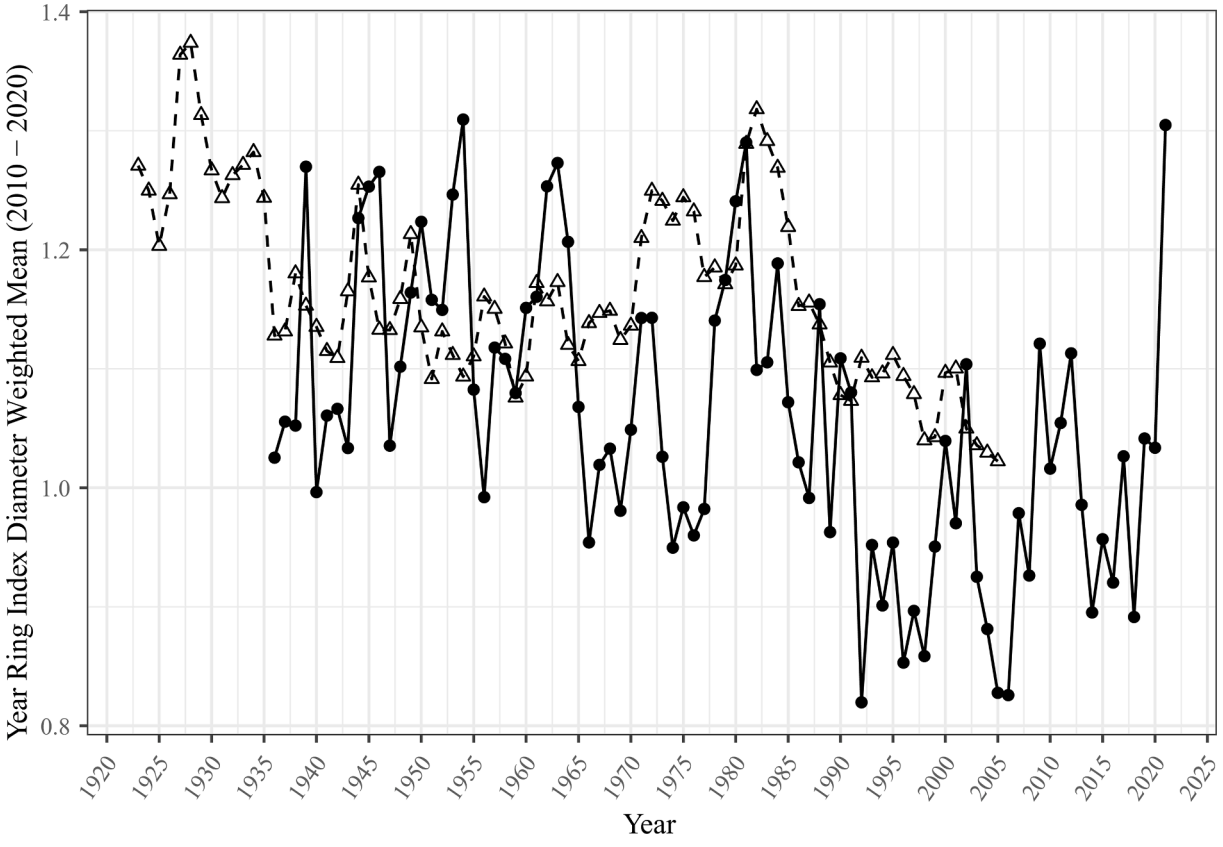

Fig. A9–1. *Q. spp.*

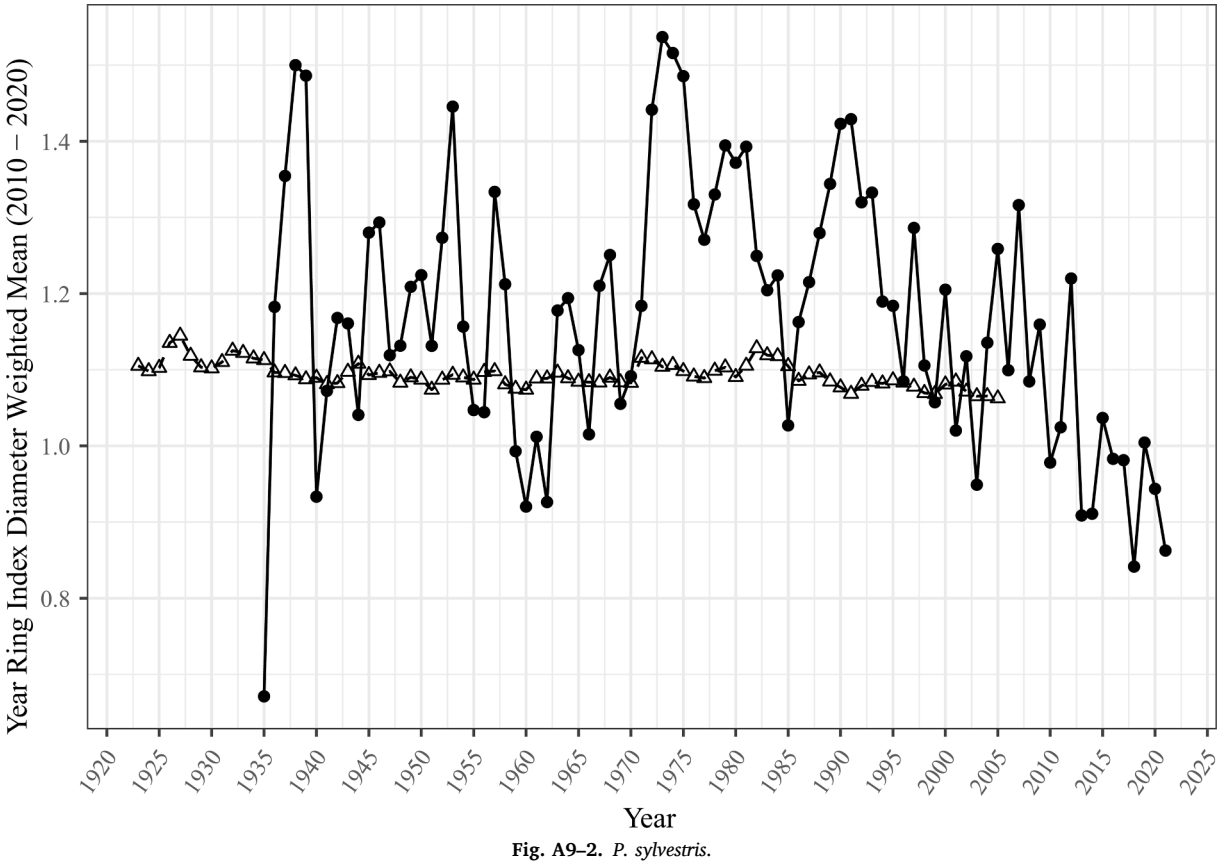

Fig. A9–2. *P. sylvestris.*

Appendix B. Supplementary data

Supplementary data to this article can be found online at https://doi.org/10.1016/j.scitotenv.2025.178858.

Data availability

Data will be made available on request.

References

Aldea, J., Dahlgren, J., Holmström, E., Löf, M., 2024. Current and future drought vulnerability for three dominant boreal tree species. Glob. Chang. Biol. 30 (1), e17079. https://doi.org/10.1111/gcb.17079.

Ameztegui, A., Cabon, A., De Caceres, M., Coll, L., 2017. Managing stand density to enhance the adaptability of scots pine stands to climate change: a modelling approach. Ecol. Model. 356, 141–150. https://doi.org/10.1016/j.ecolmodel.2017.04.006.

Argles, A.P.K., Robertson, E., Harper, A.B., Morison, J.I.L., Xenakis, G., Hastings, A., McCalmont, J., Moore, J.R., Bateman, I.J., Gannon, K., Betts, R.A., Bathgate, S., Thomas, J., Heard, M., Cox, P.M., 2023. Modelling the impact of forest management and CO2-fertilisation on growth and demography in a Sitka spruce plantation. Sci. Rep. 13 (1), 13487. https://doi.org/10.1038/s41598-023-39810-2.

Bergh, Johan, Nilsson, Urban, Kjartansson, Bjarki, Karlsson, Matts, 2010. Impact of climate change on the productivity of silver birch, Norway spruce and Scots pine stands in Sweden and economic implications for timber production. Ecol. Bull. 53, 185–196. https://www.jstor.org/stable/41442030.

Bi, D., Dix, M., Marsland, S., O'Farrell, S., Rashid, H., Uotila, P., Hirst, A., Kowalczyk, E., Golebiewski, M., Sullivan, A., Yan, H., Hannah, N., Franklin, C., Sun, Z., Vohralik, P., Watterson, I., Zhou, X., Fiedler, R., Collier, M., Puri, K., 2013. The ACCESS coupled model: description, control climate and evaluation. Australian Meteorological and Oceanographic Journal 63 (1), 41–64. https://doi.org/10.22499/2.6301.004.

Boisvenue, C., Running, S.W., 2006. Impacts of climate change on natural forest productivity—evidence since the middle of the 20th century. Glob. Chang. Biol. 12 (5). https://doi.org/10.1111/j.1365-2486.2006.01134.x. Article 5.

Bouwman, M., Forrester, D.I., Den Ouden, J., Nabuurs, G.-J., Mohren, G.M.J., 2021. Species interactions under climate change in mixed stands of scots pine and pedunculate oak. For. Ecol. Manag. 481, 118615. https://doi.org/10.1016/j.foreco.2020.118615.

Briceño-Elizondo, E., Garcia-Gonzalo, J., Peltola, H., Matala, J., Kellomäki, S., 2006. Sensitivity of growth of scots pine, Norway spruce and silver birch to climate change and forest management in boreal conditions. For. Ecol. Manag. 232 (1–3), 152–167. https://doi.org/10.1016/j.foreco.2006.05.062.

Bugmann, H., Seidl, R., Hartig, F., Bohn, F., Brůna, J., Cailleret, M., François, L., Heinke, J., Henrot, A., Hickler, T., Hülsmann, L., Huth, A., Jacquemin, I., Kollas, C., Lasch-Born, P., Lexer, M.J., Merganič, J., Merganičová, K., Mette, T., Reyer, C.P.O., 2019. Tree mortality submodels drive simulated long-term forest dynamics: assessing 15 models from the stand to global scale. Ecosphere 10 (2), e02616. https://doi.org/10.1002/ecs2.2616.

Cao, Q.V., 2014. Linking individual-tree and whole-stand models for forest growth and yield prediction. Forest Ecosystems 1 (1), 18. https://doi.org/10.1186/s40663-014-0018-z.

de Rigo, D., Caudullo, G., Houston Durrant, T., San-Miguel-Ayanz, J., 2016. In: San-Miguel-Ayanz, J., de Rigo, D., Caudullo, G., Houston Durrant, T., Mauri, A. (Eds.), The European Atlas of Forest Tree Species: Modelling, Data and Information on Forest Tree Species. European Atlas of Forest Tree Species. https://w3id.org/mtv/FISE-Comm/v01/e01aa69.

Dyderski, M.K., Paź-Dyderska, S., Jagodziński, A.M., Puchałka, R., 2025. Shifts in native tree species distributions in Europe under climate change. J. Environ. Manag. 373, 123504. https://doi.org/10.1016/j.jenvman.2024.123504.

Eaton, E., Caudullo, G., Oliveira, S., de Rigo, D., 2016. Quercus robur and Quercus petraea in Europe: Distribution, habitat, usage and threats. In: European Atlas of Forest Tree Species, vol. 14. Publications Office, pp. 160–163. https://data.europa.eu/doi/10.2760/776635.

Ekö, P.-M., 1985. En produktionsmodell för skog i Sverige, baserad på bestånd från riksskogstaxeringens provytor: A growth simulator for Swedish forests, based on data from the national forest survey.

Engel, M., Vospernik, S., Toïgo, M., Morin, X., Tomao, A., Trotta, C., Steckel, M., Barbati, A., Nothdurft, A., Pretzsch, H., Del Rio, M., Skrzyszewski, J., Ponette, Q., Löf, M., Jansons, Ā., & Brazaitis, G. (2021). Simulating the effects of thinning and species mixing on stands of oak (*Quercus petraea* (Matt.) Liebl./*Quercus robur* L.) and pine (*Pinus sylvestris* L.) across Europe. Ecol. Model., 442, 109406. doi:https://doi.org/10.1016/j.ecolmodel.2020.109406.

European Union, 2023. Regulation (EU) 2023/839 amending regulation (EU) 2018/841. Off. J. Eur. Union. L 107, 1–28. http://data.europa.eu/eli/reg/2023/839/oj.

Fontes, L., Bontemps, J.-D., Bugmann, H., Van Oijen, M., Gracia, C., Kramer, K., Lindner, M., Rötzer, T., Skovsgaard, J.P., 2010. Models for supporting forest management in a changing environment. Forest Systems 19, 8–29. https://doi.org/10.5424/fs/201019S-9315.

Forrester, David I., Tang, Xiaolu, 2016. Analysing the spatial and temporal dynamics of species interactions in mixed-species forests and the effects of stand density using the 3-PG model. Ecol. Model. 319, 233–254. https://doi.org/10.1016/j.ecolmodel.2015.07.010.

García, O., 2017. Cohort aggregation modelling for complex forest stands: spruce–aspen mixtures in British Columbia. Ecol. Model. 343, 109–122. https://doi.org/10.1016/j.ecolmodel.2016.10.020.

Goberville, E., Beaugrand, G., Hautekèete, N., Piquot, Y., Luczak, C., 2015. Uncertainties in the projection of species distributions related to general circulation models. Ecol. Evol. 5 (5), 1100–1116. https://doi.org/10.1002/ece3.1411.

Goude, M., Nilsson, U., Mason, E., Vico, G., 2022. Using hybrid modelling to predict basal area and evaluate effects of climate change on growth of Norway spruce and scots pine stands. Scand. J. For. Res. 37 (1), 59–73. https://doi.org/10.1080/02827581.2022.2039278.

Gutsch, M., Lasch-Born, P., Suckow, F., Reyer, C.P.O., 2016. Evaluating the productivity of four main tree species in Germany under climate change with static reduced models. Ann. For. Sci. 73 (2), 401–410. https://doi.org/10.1007/s13595-015-0532-3.

Hartig, F. (n.d.). *DHARMa: residual diagnostics for hierarchical (multi-level / mixed) regression models.* (version 0.4.6) [R; Winx86-64]. https://CRAN.R-project.org/package=DHARMa.

Hartigan, J.A., Wong, M.A., 1979. Algorithm AS 136: a K-means clustering algorithm. Appl. Stat. 28 (1), 100. https://doi.org/10.2307/2346830.

Hasenauer, H., Monserud, R.A., 1996. A crown ratio model for Austrian forests. For. Ecol. Manag. 84 (1–3), 49–60. https://doi.org/10.1016/0378-1127(96)03768-1.

Hastie, T., Tibshirani, R., 1986. Generalized additive models. Stat. Sci. 1 (3), 297–318.

IPCC, 2013. Annex II: Climate system scenario tables. In: Stocker, T.F., Qin, D., Plattner, G.-K., Tignor, M., Allen, S.K., Boschung, J., Nauels, A., Xia, Y., Bex, V., Midgley, P.M. (Eds.), *Climate Change 2013: The Physical Science Basis. Contribution of Working Group I to the Fifth Assessment Report of the Intergovernmental Panel on Climate Change* (Pp. 1395–1446). Cambridge University Press. https://doi.org/10.1017/CBO9781107415324.030.

Jonard, M., Fürst, A., Verstraeten, A., Thimonier, A., Timmermann, V., Potočić, N., Waldner, P., Benham, S., Hansen, K., Merilä, P., Ponette, Q., De La Cruz, A.C., Roskams, P., Nicolas, M., Croisé, L., Ingerslev, M., Matteucci, G., Decinti, B., Bascietto, M., Rautio, P., 2015. Tree mineral nutrition is deteriorating in Europe. Glob. Chang. Biol. 21 (1), 418–430. https://doi.org/10.1111/gcb.12657.

Kahn, M., 1994. Modellierung der Höhenentwicklung ausgewählter Baumarten in Abhängigkeit vom Standort. Forstliche Forschungsberichte München. Band, 141, 204 pages.

Karger, D. N., Schmatz, D., Dettling, G., & Zimmermann, N. E. (2019). *High resolution monthly precipitation and temperature timeseries for the period 2006-2100* (version 1.0) [netCDF4]. EnviDat. Doi:10.16904/ENVIDAT.124.

Karger, D.N., Schmatz, D.R., Dettling, G., Zimmermann, N.E., 2020. High-resolution monthly precipitation and temperature time series from 2006 to 2100. Scientific Data 7 (1). https://doi.org/10.1038/s41597-020-00587-y. Article 1.

Kauppi, P.E., Stål, G., Arnesson-Ceder, L., Hallberg Sramek, I., Hoen, H.F., Svensson, A., Wernick, I.K., Högberg, P., Lundmark, T., Nordin, A., 2022. Managing existing forests can mitigate climate change. For. Ecol. Manag. 513, 120186. https://doi.org/10.1016/j.foreco.2022.120186.

Kellomäki, S., Väisänen, H., 1997. Modelling the dynamics of the forest ecosystem for climate change studies in the boreal conditions. Ecol. Model. 97 (1–2), 121–140. https://doi.org/10.1016/S0304-3800(96)00081-6.

Kellomäki, S., Peltola, H., Nuutinen, T., Korhonen, K.T., Strandman, H., 2008. Sensitivity of managed boreal forests in Finland to climate change, with implications for adaptive management. Philos. Trans. R. Soc. B 363 (1501), 2339–2349. https://doi.org/10.1098/rstb.2007.2204.

Kellomäki, S., Strandman, H., Heinonen, T., Asikainen, A., Venäläinen, A., Peltola, H., 2018. Temporal and spatial change in diameter growth of boreal scots pine, Norway spruce, and birch under recent-generation (CMIP5) global climate model projections for the 21st century. Forests 9 (3), 118. https://doi.org/10.3390/f9030118.

Landsberg, J.J., Waring, R.H., 1997. A generalised model of forest productivity using simplified concepts of radiation-use efficiency, carbon balance and partitioning. For. Ecol. Manag. 95 (3), 209–228. https://doi.org/10.1016/S0378-1127(97)00026-1.

Lindner, M., Fitzgerald, J.B., Zimmermann, N.E., Reyer, C., Delzon, S., Van Der Maaten, E., Schelhaas, M.-J., Lasch, P., Eggers, J., Van Der Maaten-Theunissen, M., Suckow, F., Psomas, A., Poulter, B., Hanewinkel, M., 2014. Climate change and European forests: what do we know, what are the uncertainties, and what are the implications for forest management? J. Environ. Manag. 146, 69–83. https://doi.org/10.1016/j.jenvman.2014.07.030.

Lindsay, K., Bonan, G.B., Doney, S.C., Hoffman, F.M., Lawrence, D.M., Long, M.C., Mahowald, N.M., Keith Moore, J., Randerson, J.T., Thornton, P.E., 2014. Preindustrial-control and twentieth-century carbon cycle experiments with the earth system model CESM1(BGC). J. Clim. 27 (24), 8981–9005. https://doi.org/10.1175/JCLI-D-12-00565.1.

Mäkinen, H., Yue, C.F., Kohnle, U., 2017. Site index changes of scots pine, Norway spruce and larch stands in southern and Central Finland. Agric. For. Meteorol. 237, 95–104. https://doi.org/10.1016/j.agrformet.2017.01.017.

Matías, L., Linares, J.C., Sánchez-Miranda, Á., Jump, A.S., 2017. Contrasting growth forecasts across the geographical range of scots pine due to altitudinal and

latitudinal differences in climatic sensitivity. Glob. Chang. Biol. 23 (10), 4106–4116. https://doi.org/10.1111/gcb.13627.
Mauri, A., Girardello, M., Forzieri, G., Manca, F., Beck, P.S.A., Cescatti, A., Strona, G., 2023. Assisted tree migration can reduce but not avert the decline of forest ecosystem services in Europe. Glob. Environ. Chang. 80, 102676. https://doi.org/10.1016/j.gloenvcha.2023.102676.
Mensah, A.A., Holmström, E., Nyström, K., Nilsson, U., 2022. Modelling potential yield capacity in conifers using Swedish long-term experiments. For. Ecol. Manag. 512, 120162. https://doi.org/10.1016/j.foreco.2022.120162.
Monserud, R.A., Sterba, H., 1999. Modeling individual tree mortality for Austrian forest species. For. Ecol. Manag. 113 (2–3), 109–123. https://doi.org/10.1016/S0378-1127(98)00419-8.
Morin, X., Augspurger, C., Chuine, I., 2007. Process-based modeling of species' distributions: what limits temperate tree species' range boundaries? Ecology 88 (9), 2280–2291. https://doi.org/10.1890/06-1591.1.
Nachtmann, G., 2005. Der Höhenzuwachs österreichischer Baumarten in Abhängigkeit von Standort und Konkurrenz [PhD Thesis].. BOKU.
Nemani, R.R., Keeling, C.D., Hashimoto, H., Jolly, W.M., Piper, S.C., Tucker, C.J., Myneni, R.B., Running, S.W., 2003. Climate-driven increases in global terrestrial net primary production from 1982 to 1999. Science 300 (5625), 1560–1563. https://doi.org/10.1126/science.1082750.
Newnham, R.M., 1964. *The development of a stand model for Douglas fir* (version 1) [Diss., University of British Columbia]. https://doi.library.ubc.ca/10.14288/1.0105410.
NOAA, 2024. THE NOAA ANNUAL GREENHOUSE GAS INDEX (AGGI). https://gml.noaa.gov/aggi/aggi.html (Updated Summer).
Nölte, A., Yousefpour, R., Hanewinkel, M., 2020. Changes in sessile oak (Quercus petraea) productivity under climate change by improved leaf phenology in the 3-PG model. Ecol. Model. 438, 109285. https://doi.org/10.1016/j.ecolmodel.2020.109285.
Norby, R.J., DeLucia, E.H., Gielen, B., Calfapietra, C., Giardina, C.P., King, J.S., Ledford, J., McCarthy, H.R., Moore, D.J.P., Ceulemans, R., De Angelis, P., Finzi, A.C., Karnosky, D.F., Kubiske, M.E., Lukac, M., Pregitzer, K.S., Scarascia-Mugnozza, G.E., Schlesinger, W.H., Oren, R., 2005. Forest response to elevated CO $_2$ is conserved across a broad range of productivity. Proc. Natl. Acad. Sci. 102 (50), 18052–18056. https://doi.org/10.1073/pnas.0509478102.
Paterson, S., 1956. The Forest Area of the World and its Potential Productivity. Göteborgs Univ. Geografiska Inst, Medd, p. 51.
Petersson, H., Ellison, D., Appiah Mensah, A., Berndes, G., Egnell, G., Lundblad, M., Lundmark, T., Lundström, A., Stendahl, J., Wikberg, P., 2022. On the role of forests and the forest sector for climate change mitigation in Sweden. GCB Bioenergy 14 (7), 793–813. https://doi.org/10.1111/gcbb.12943.
Petit, R.J., Bodénès, C., Ducousso, A., Roussel, G., Kremer, A., 2004. Hybridization as a mechanism of invasion in oaks. New Phytol. 161 (1), 151–164. https://doi.org/10.1046/j.1469-8137.2003.00944.x.
Pretzsch, H., Biber, P., Schütze, G., Uhl, E., Rötzer, T., 2014. Forest stand growth dynamics in Central Europe have accelerated since 1870. *Nature*. Communications 5 (1). https://doi.org/10.1038/ncomms5967. Article 1.
Pretzsch, H., Steckel, M., Heym, M., Biber, P., Ammer, C., Ehbrecht, M., Bielak, K., Bravo, F., Ordóñez, C., Collet, C., Vast, F., Drössler, L., Brazaitis, G., Godvod, K., Jansons, A., de-Dios-García, J., Löf, M., Aldea, J., Korboulewsky, N., del Río, M., 2020. Stand growth and structure of mixed-species and monospecific stands of Scots pine (*Pinus sylvestris* L.) and oak (*Q. robur* L., Quercus petraea (Matt.) Liebl.) analysed along a productivity gradient through Europe. Eur. J. For. Res. *139* (3), 349–367. https://doi.org/10.1007/s10342-019-01233-y.
Pretzsch, H., Del Río, M., Arcangeli, C., Bielak, K., Dudzinska, M., Forrester, D.I., Klädtke, J., Kohnle, U., Ledermann, T., Matthews, R., Nagel, J., Nagel, R., Ningre, F., Nord-Larsen, T., Biber, P., 2023a. Forest growth in Europe shows diverging large regional trends. Sci. Rep. 13 (1), 15373. https://doi.org/10.1038/s41598-023-41077-6.
Pretzsch, Hans, Heym, Michael, Hilmers, Torben, Bravo-Oviedo, Andrés, Ahmed, Shamim, Ammer, Christian, Avdagić, Admir, Bielak, Kamil, Bravo, Felipe, Brazaitis, Gediminas, Fabrika, Marek, Hurt, Vaclav, Kurylyak, Viktor, Löf, Magnus, Pach, Maciej, Ponette, Quentin, Ruiz-Peinado, Ricardo, Stojanovic, Dejan, Svoboda, Miroslav, Wolff, Barbara, Zlatanov, Tzvetan, del Río, Miren, 2023b. Mortality reduces overyielding in mixed Scots pine and European beech stands along a precipitation gradient in Europe. For. Ecol. Manage. ISSN: 0378-1127 539, 121008. https://doi.org/10.1016/j.foreco.2023.121008 (https://www.sciencedirect.com/science/article/pii/S0378112723002426).
Sanderson, B.M., Knutti, R., Caldwell, P., 2015. A representative democracy to reduce interdependency in a multimodel ensemble. J. Clim. 28 (13), 5171–5194. https://doi.org/10.1175/JCLI-D-14-00362.1.
Scoccimarro, E., Gualdi, S., Bellucci, A., Sanna, A., Giuseppe Fogli, P., Manzini, E., Vichi, M., Oddo, P., Navarra, A., 2011. Effects of tropical cyclones on ocean heat transport in a high-resolution coupled general circulation model. J. Clim. 24 (16), 4368–4384. https://doi.org/10.1175/2011JCLI4104.1.
Shukla, P. R., Skea, J., Slade, R., van Diemen, R., Haughey, E., Malley, J., Pathak, M., & Portugal Pereira, J. (Eds.). (2019). Technical Summary. In P. R. Shukla, J. Skea, E. Calvo Buendia, V. Masson-Delmotte, H-O. Pörtner, D. C. Roberts, P. Zhai, R. Slade, S. Connors, R. van Diemen, M. Ferrat, E. Haughey, S. Luz, S. Neogi, M. Pathak, J. Petzold, J. Portugal Pereira, P. Vyas, E. Huntley, … J. Malley (Eds.), *Climate Change and Land: An IPCC special report on climate change, desertification, land degradation, sustainable land management, food security, and greenhouse gas fluxes in terrestrial ecosystems* (p. 45). doi:https://doi.org/10.1017/9781009157988.002.
Simpson, G., 2024. January 24. Non-normal random effects in a logistic GAM. https://stats.stackexchange.com/q/380159. https://stats.stackexchange.com/users/1390/gavin-simpson.
Skytt, T., Englund, G., Jonsson, B.-G., 2021. Climate mitigation forestry—temporal trade-offs. Environ. Res. Lett. 16 (11), 114037. https://doi.org/10.1088/1748-9326/ac30fa.
Sperry, J.S., Venturas, M.D., Todd, H.N., Trugman, A.T., Anderegg, W.R.L., Wang, Y., Tai, X., 2019. The impact of rising CO $_2$ and acclimation on the response of US forests to global warming. Proc. Natl. Acad. Sci. 116 (51), 25734–25744. https://doi.org/10.1073/pnas.1913072116.
Steckel, M., del Río, M., Heym, M., Aldea, J., Bielak, K., Brazaitis, G., Černý, J., Coll, L., Collet, C., Ehbrecht, M., Jansons, A., Nothdurft, A., Pach, M., Pardos, M., Ponette, Q., Reventlow, D.O.J., Sitko, R., Svoboda, M., Vallet, P., Pretzsch, H., 2020. Species mixing reduces drought susceptibility of scots pine (Pinus sylvestris L.). and oak (Quercus robur L., Quercus petraea (Matt.) Liebl.) – Site water supply and fertility modify the mixing effect For. Ecol. Manag. 461, 117908. https://doi.org/10.1016/j.foreco.2020.117908.
Taylor, K.E., Stouffer, R.J., Meehl, G.A., 2012. An overview of CMIP5 and the experiment design. Bull. Am. Meteorol. Soc. 93 (4), 485–498. https://doi.org/10.1175/BAMS-D-11-00094.1.
Terrer, C., Vicca, S., Stocker, B.D., Hungate, B.A., Phillips, R.P., Reich, P.B., Finzi, A.C., Prentice, I.C., 2018. Ecosystem responses to elevated CO $_2$ governed by plant–soil interactions and the cost of nitrogen acquisition. New Phytol. 217 (2), 507–522. https://doi.org/10.1111/nph.14872.
UNFCCC, 1992. United Nations Framework Convention On Climate Change (FCCC/INFORMAL/84.GE.05-62220 (E) 200705; p. 24). Secretariat of the United Nations Framework Convention on Climate Change. https://www.ipcc.ch/apps/njlite/srex/njlite_download.php?id=5592.
UNFCCC, 2021. Agenda item 2(c): draft decision -/CMA.3: Glasgow climate pact. Organization of Work, Including for the Sessions of the Subsidiary Bodies 10. https://unfccc.int/sites/default/files/resource/cma2021_L16_adv.pdf.
Vallet, P., Perot, T., 2018. Coupling transversal and longitudinal models to better predict Quercus petraea and Pinus sylvestris stand growth under climate change. Agric. For. Meteorol. 263, 258–266. https://doi.org/10.1016/j.agrformet.2018.08.021.
Vospernik, S., 2021. Basal area increment models accounting for climate and mixture for Austrian tree species. For. Ecol. Manag. 480, 118725. https://doi.org/10.1016/j.foreco.2020.118725.
Vospernik, S., Monserud, R.A., Sterba, H., 2010. Do individual-tree growth models correctly represent height:diameter ratios of Norway spruce and scots pine? For. Ecol. Manag. 260 (10), 1735–1753. https://doi.org/10.1016/j.foreco.2010.07.055.
Vospernik, S., Heym, M., Pretzsch, H., Pach, M., Steckel, M., Aldea, J., Brazaitis, G., Bravo-Oviedo, A., Del Rio, M., Löf, M., Pardos, M., Bielak, K., Bravo, F., Coll, L., Černý, J., Droessler, L., Ehbrecht, M., Jansons, A., Korboulewsky, N., Wolff, B., 2023. Tree species growth response to climate in mixtures of Quercus robur/Quercus petraea and Pinus sylvestris across Europe—a dynamic, sensitive equilibrium. For. Ecol. Manag. 530, 120753. https://doi.org/10.1016/j.foreco.2022.120753.
Vospernik, Sonja, Vigren, Carl, Morin, Xavier, Toïgo, Maude, Bielak, Kamil, Brazaitis, Gediminas, Bravo, Felipe, Heym, Michael, del Río, Miren, Jansons, Aris, Löf, Magnus, Nothdurft, Arne, Pardos, Marta, Pach, Maciej, Ponette, Quentin, Pretzsch, Hans, 2024. Can mixing Quercus robur and Quercus petraea with Pinus sylvestris compensate for productivity losses due to climate change? Sci. Total Environ. ISSN: 0048-9697 942, 173342. https://doi.org/10.1016/j.scitotenv.2024.173342 (https://www.sciencedirect.com/science/article/pii/S0048969724034892).
Watanabe, M., Suzuki, T., O'ishi, R., Komuro, Y., Watanabe, S., Emori, S., Takemura, T., Chikira, M., Ogura, T., Sekiguchi, M., Takata, K., Yamazaki, D., Yokohata, T., Nozawa, T., Hasumi, H., Tatebe, H., & Kimoto, M., 2010. Improved climate simulation by MIROC5: mean states, variability, and climate sensitivity. J. Clim. 23 (23), 6312–6335. https://doi.org/10.1175/2010JCLI3679.1.
Wessely, J., Essl, F., Fiedler, K., Gattringer, A., Hülber, B., Ignateva, O., Moser, D., Rammer, W., Dullinger, S., Seidl, R., 2024. A climate-induced tree species bottleneck for forest management in Europe. Nature Ecology & Evolution 8 (6), 1109–1117. https://doi.org/10.1038/s41559-024-02406-8.
Wood, S.N., 2011. Fast stable restricted maximum likelihood and marginal likelihood estimation of semiparametric generalized linear models: estimation of semiparametric generalized linear models. J. R. Stat. Soc. https://doi.org/10.1111/j.1467-9868.2010.00749.x. Series B (Statistical Methodology), 73(1), Article 1.